Biologics: Targets and Therapy

Dovepress
Taylor & Francis Group

Open Access Full Text Article

ORIGINAL RESEARCH

Boswellia carteri Birdw. Resin Extract Induces Phase-I Cytochrome P-450 Enzyme Gene Expressions in Human Hepatocarcinoma (Hep G2) Cells: In vitro and in silico Studies

Sahar S Alghamdi[1–3], Hussah N Albahlal[1], Raghad Saleh Alajmi[1], Amani Alsharidah[4], Aljawharah Almogren[2], Rasha Suliman[5], Zeyad I Alehaideb[1–3]

[1]King Saud Bin Abdulaziz University for Health Sciences (KSAU-HS), Riyadh, Saudi Arabia; [2]King Abdullah International Medical Research Center (KAIMRC), Riyadh, Saudi Arabia; [3]Ministry of National Guard Health Affairs (MNGHA), Riyadh, Saudi Arabia; [4]King Saud University (KSU), Riyadh, Saudi Arabia; [5]Fatima College for Health Sciences, Abu Dhabi, United Arab Emirates

Correspondence: Sahar S Alghamdi, Email ghamdisa@ksau-hs.edu.sa

Introduction: *Boswellia carteri* (*B. carteri*) resin is widely recognized for its anti-inflammatory, wound-healing, and immunomodulatory properties. This study examines the ability of its aqueous extracts to modulate the expression of key cytochrome P450 (CYP) enzymes—CYP1A2, CYP2B6, and CYP3A4—in Hep G2 cells, emphasizing pharmacokinetic and toxicological implications.

Methods: Aqueous extracts were evaluated for endotoxin contamination and cytotoxicity to ensure suitability for in vitro experimentation. PCR analysis was employed to quantify CYP enzyme gene expression. Computational tools, including Protox-II, Swiss ADME, and molecular docking, were used to assess pharmacokinetics, CYP interactions, and biological targets. Competitive binding assays were performed to investigate the involvement of the constitutive androstane receptor (CAR) in CYP induction.

Results: The results suggest that several metabolites, particularly ursodeoxycholic acid and beta-sitosterol, show potential interactions with CYP enzymes, with ursodeoxycholic acid demonstrating the highest probability of biological effects on CYP and a strong binding affinity to the Constitutive Androstane Receptor (CAR). Moreover, a receptor competitive binding assay suggested that the primary mechanism of CYP 2B6 and 3A4 induction is through activation of the CAR receptor although additional confirmatory studies are necessary.

Discussion: The observed CYP enzyme induction through CAR receptor activation aligns with USFDA guidelines for CYP studies. However, the hepatotoxic potential of ursodeoxycholic acid and the associated toxicity risks of other metabolites underscore the need for caution. The findings highlight the potential for herb–drug interactions, particularly with pharmaceuticals metabolized by CYP enzymes.

Conclusion: In conclusion, there is a potential for interactions between *B. carteri* resins and pharmaceuticals metabolized by CYP enzymes; thus, we advise caution to consumers, patients, and healthcare providers regarding their concomitant use. Although our findings provide valuable insights, further in vivo studies are essential to validate the modulatory effects of *B. carteri* on CYP gene expression.

Keywords: *Boswellia carteri*, cytochrome P-450 enzymes, nuclear receptors, natural products, oleo-gum resin

Introduction

The plant genus *Boswellia* (*B).*, belongs to the *Burseraceae* family of plants, which comprises twenty species including the three important species of *B. serrata* Roxb., *B. frereana* Birdw., and *B. carteri* Birdw. to name a few. *B. carteri* (synonym: *B. sacra* Flueck) frankincense trees is endemic to the Southern Arabian Peninsula and African horn regions.[1] The oleo-gum resins of *B. carteri*, also known as Luban (in Arabic, لبان) are used by the populations for their cosmetic and medicinal properties.[2] The resins are prepared and consumed as a decoction, infusion, or raw resin form and are

Received: 13 August 2024
Accepted: 11 January 2025
Published: 5 May 2025

© 2025 Alghamdi et al. This work is published and licensed by Dove Medical Press Limited. The full terms of this license are available at https://www.dovepress.com/terms.php and incorporate the Creative Commons Attribution – Non Commercial (unported, v4.0) License (http://creativecommons.org/licenses/by-nc/4.0/). By accessing the work you hereby accept the Terms. Non-commercial uses of the work are permitted without any further permission from Dove Medical Press Limited, provided the work is properly attributed. For permission for commercial use of this work, please see paragraphs 4.2 and 5 of our Terms (https://www.dovepress.com/terms.php).

Graphical Abstract

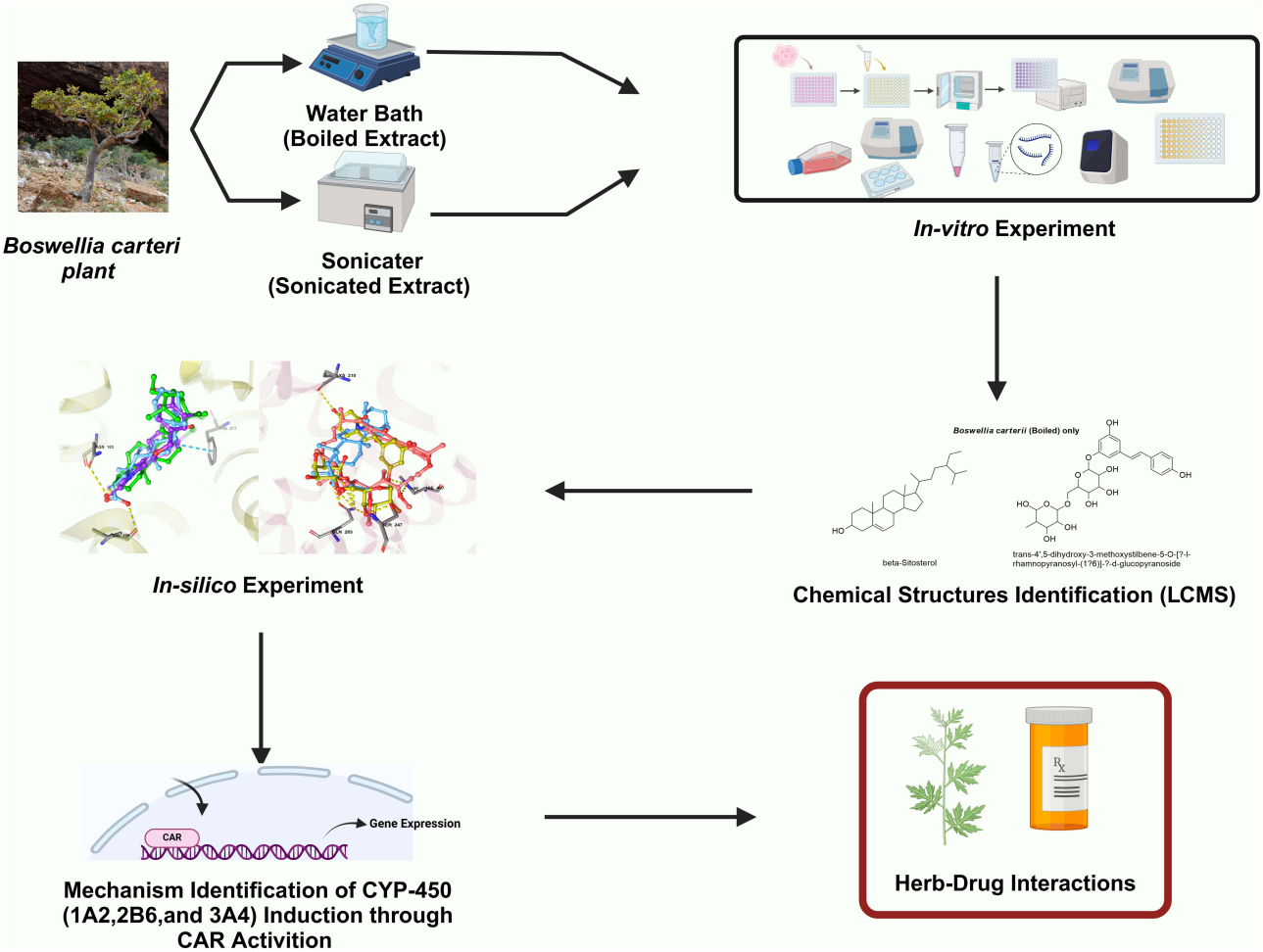

reported to treat inflammatory conditions (eg, rheumatoid arthritis, asthma, osteoarthritis), as well as some cancerous diseases, wound healing, and antimicrobial properties.[3] The *B. carteri* resins were found to contain mono-, sesqui-, di-, triterpenoids and water-soluble gum with numerous pharmacological activities.[4] The triterpenoids in *B. carteri* resins were found to have immunomodulatory properties.[5] The resins were found to have antimicrobial, anti-insect, and wound-healing properties.[6,7] Although scarce, few studies have reported the consumption of *B. carteri* resin among patients. For example, a survey reported that 60% of 102 patients with allergic disorders consumed herbal medicines, including 11.8% who consumed *B. carteri* resin.[8] In another study, a survey reported that 56% of 308 patients used herbal medicines, including *B. carteri* resins. Respiratory, gastrointestinal, and endocrine disorders were the most prescribed for indications.[9] Despite the relative popularity of *B. carteri* resin consumption by patients, no studies have determined whether the repeated consumption of such resins can modulate the expression of important metabolic enzymes in humans.

After oral consumption, pharmaceutical drugs undergo several phases including absorption, distribution, metabolism, and excretion (ADME). Most herb–drug interactions involve the alteration of one or more pharmacokinetic phases, most notably the alteration of the metabolism of a pharmaceutical drug, during the concomitant consumption of natural products, such as herbal medicines.[10] The main enzyme system involved in pharmaceutical drug metabolism is the phase-I Cytochrome P-450 (CYP) family, which comprises numerous isoenzymes involved in xenobiotic drug

metabolism.[11] Once exposed to xenobiotics, these enzymes are subjected to inhibition and induction, once exposed to xenobiotic(s), which can lead to serious drug adverse effects in sensitive patients.[12] The induction of CYP isoenzymes is mainly mediated by nuclear receptors, especially Pregnane X Receptor (PXR), Constitutive Androstane Receptor (CAR), and Aryl Hydrocarbon Receptor (AhR).[13] These ligand-activated transcription factors, located in the cell cytoplasm, translocate to the nucleus and bind to Deoxyribonucleic Acid (DNA) response elements, leading to the upregulation of metabolic enzymes (ie, CYP) and transporter (ie, multidrug resistance-associated protein) expression.[14]

The main objectives of this study were (1) to determine whether treatment with *B. carteri* resins, in boiled and sonicated forms, could modulate the expression of three important CYP enzymes, including CYP 1A2, 2B6, and 3A4, in Hep G2 cells using a series of in vitro studies; (2) to tentatively identify the secondary phytochemical metabolites in boiled and sonicated aqueous extracts of *B. carteri* resin using Liquid Chromatography and Mass Spectrometry (LC/MS); (3) to perform in silico molecular studies and docking involving the identified *B. carteri* derived metabolites against the crystal structures of human PXR and CAR; and (4) to perform PXR and CAR receptor binding assays to complement the findings of the in silico molecular docking study.

Materials and Methods

Materials and Chemicals

Dulbecco's Modified Eagle Medium (DMEM) plus GlutaMax-1 1X (4.5g/l D-Glucose, 25 mm HEPES, Pyruvate), Fetal Bovine Serum (FBS), TrypLE™ Express, and Dulbecco's Phosphate-Buffered Saline (PBS) were obtained from Gibco® (Waltham, MA). Rifampicin (USP grade, ≥97%) was obtained from UFC Biotechnology Fine Chemicals (Amherst, NY, USA). Dimethyl Sulfoxide (DMSO) (99.9% purity) was obtained from Calbiochem (San Diego, CA). Purified Carbon Dioxide (CO_2) gas was obtained from Saudi Industrial Gas (Dammam, Saudi Arabia). Ultrapure water was produced using a Millipore (Billerica, MA) system with a resistivity reading of 18.2 MΩ·cm at 25°C.

Source of B. carteri Resins

The resins were obtained from Boswellness (Colchester, VT) with product number BC000109. The resins were certified as organic and free of alterations, pesticides, and preservatives, as they were wildcrafted in the Federal Republic of Somalia by experts. The resins were stored in a cool and dark area until processing. The remaining resin sample was stored in our institution for future studies.

Extraction of B. carteri Resins

Prior to extraction, the resins of *B. carteri* were finely powered using a typical electric grinder. For sonicated extraction, approximately 500 mg of the fine powder was mixed with 10.0 mL of ultra-pure water and sonicated for 30 min in high-power mode using an ultrasonic water bath. For boiling water, approximately 500 mg of resin was mixed with 10.0 mL of ultra-pure water and boiled until half of the volume evaporated. The extracts were filtered using a Sartorius Stedim biotech (Göttingen, Germany) quantitative ashless paper filter and completely dried in a Thermo Fisher Scientific (Waltham, MA, USA) SAVANT SpeedVac Concentrator. The remaining dried pellets were weighed and reconstituted in 0.5 mL of DMSO by vertexing until they were completely dissolved. The reconstituted extracts were stored at cool temperatures in the dark until use.

Endotoxin Measurement in Aqueous Extracts of B. carteri Resins

The levels of endotoxin contamination in *B. carteri* resin aqueous extracts were measured using a Thermo Scientific Pierce Chromogenic Endotoxin Quant kit (catalog number, A39553) according to the manufacturer's instructions.

Source of Hep G2 Cells

Human Hepatocellular Carcinoma (Hep G2) cells were obtained from the American Type Culture Collection (Manassas, VA). These cells were derived from a 15-year-old male Caucasian adolescent patient diagnosed with hepatocellular carcinoma.

Hep G2 Cell Culture

Hep G2 cells were cultured in complete DMEM GlutaMAX medium containing 10% (*v/v*) FBS, and one percent (*v/v*) penicillin G (100 IU/mL), and streptomycin (100 µg/mL) and incubated at 37°C in five percent CO_2 and 95% humidity. The medium was changed 2 to 3 days, and the cells were sub-cultured when the cell population density reached 70–80% confluency. The cells were seeded at an appropriate density according to each experimental design. For the cell viability experiment, concentrations used ranged from 0.03 to 546 µg dry extract weight per mL for sonicated extract and 0.02 to 305 µg dry extract weight per mL for boiled extract. For gene expression assessment, Hep G2 cells were treated with three different concentrations of boiled and sonicated aqueous *B. carteri* extracts (25, 50, and 100 µg/mL) for each boiled and sonicated aqueous *B. carteri* extract. Rifampicin was used as a positive control at 1.0 µM concentration.

Measurement of Hep G2 Viability by MTT Assay

The antiproliferative effects of boiled and sonicated aqueous extracts of *B. carteri* resins on Hep G2 cell proliferation were determined to aid in the selection of extract concentrations for further downstream experiments using the Sigma-Aldrich (St. Louis, MO, USA) 3-[4,5-dimethylthiazol-2-yl]-2,5-diphenyltetrazolium bromide (MTT) assay-based cell growth determination kit (catalog number, CGD-1). Briefly, previously seeded in 96-well plates, treated and untreated Hep G2 cells, at a density of 4×10^3 cells per well, were incubated for 48 hrs then addition of a 10% MTT solution for 3 hrs at 37°C. The MTT solution was replaced with an equal volume of isopropanol. The plates were shaken for 45 min at room temperature. Absorbance was measured at 560 nm using a BioTek Instruments Universal Microplate Reader ELx800 counter (Winooski, VT, USA).

Ribonucleic Acid (RNA) Extraction from Untreated and Treated Hep G2 Cells

The treated and untreated Hep G2 cells were washed three times with PBS and harvested using the TrypLE™ Express solution. The cells were transferred to a 1.5 mL tube and centrifuged at 15,000 rpm for 5 min to obtain pellets that were stored at −20°C until use. The whole RNA was extracted from treated and untreated cell pellets using the Qiagen (Hilden, Germany) RNeasy Plus Mini kit (catalog number, 74106) as per the manufacturer's instructions.

Measurement of CYP 1A2, 2B6, and 3A4 Gene Expression by q-PCR Technique

The CYP gene expression measurement method used was based on[15] with modifications[16]. Briefly, complementary DNA (cDNA), at 50.0 ng per well, was first produced from the whole RNA extract via reverse transcription using the Applied Biosystems (Waltham, MA) High-Capacity cDNA Reverse Transcription kit (catalog number, 4368813) according to the manufacturer's instructions. Quantitative real-time PCR (qPCR) was performed using a Thermo Fisher Scientific SYBR Green PCR Master Mix kit (catalog number: 4309155) and performed on an Applied Biosystems 7900 Real-Time PCR System. For each analysis, a negative control was prepared using all reagents, except the cDNA template. The house-keeping gene glyceraldehyde-3-phosphate dehydrogenase (GAPDH) was used as an internal control and cytochrome enzyme primers were used at 10.0 pmol/µL concentration as listed in Table 1.

Identification of Secondary Metabolites in B. carteri Aqueous Extracts Using Liquid Chromatography and Mass Spectrometry (LCMS) Technique

The method of identification of *B. carteri* resin-derived metabolites was performed using an Agilent (Santa Clara, CA) 1260 Infinity High-Performance Liquid Chromatography system coupled to Agilent 6530 Q-TOF as described.[16] Briefly, the separation was first performed using an Agilent SB-C18 column (4.6 mm × 150 mm, 1.8 µm) with the elution gradient program as follows: 0 to 2 min, 5% B, 2 to 17 min, 5 to 100% B; 17 to 21 min, 95% B; 21 to 25 min, 5% B,

Table 1 The List of CYP Primer Sequences

Supplier	Gene	Sequence	Amplicon Size (bp)
Macrogen	CYP-2B6-F1	CCAACATACCAGATCCGCTTCCTG	205
Macrogen	CYP-2B6-R1	CCTGCACTCACTTGCAATGTGACC	
Macrogen	CYP-1A2-F1	CAGAATGCCCTCAACACCTTCTCC	269
Macrogen	CYP-1A2-R1	GCAGTCTCCACGAACTCATGAGT	
Macrogen	CYP-3A4-F	GGATGTTGAAGTGAGCTGAGATTGC	228
Macrogen	CYP-3A4-R	GGTGTTGAGGATGGAATGCAAGAG	
Macrogen	GAPDH -F	CCAGGGCTGCTTTTAACTCTGG	244
Macrogen	GAPDH- R	CCAGTGGACTCCACGACGTAC	

using mobile-phase A (0.1% formic acid in water) and mobile-phase B (0.1% formic acid in methanol). The flow rate was set at 250 µL/minand the injection volume was 10 µL. The gas temperature was set at 300 °C; gas flow at 8 L/min; nebulizer pressure at 35 psi; sheath gas flow rate at 11 L/min; gas temperature at 350 °C; and scanning range was 50–800 mass-to-charge (*m/z*). The data were generated using Agilent MassHunter (version B.06.00) analysis software.

In silico Prediction

Biological Activity (Prediction of Activity Spectra for Substances (PASS) Web Server)

PASS Online (https://www.way2drug.com/passonline/) predicts the biological effects of organic metabolites, achieving an average accuracy of over 95% for more than 4000 distinct categories of biological activity, based on their structural formulas. To construct the PASS prediction tool, 19,000 primary chemicals obtained from the MDL Drug Data Report database are used in the construction of the PASS prediction tool.[17] Furthermore, the PASS Online web server differs from Super-PRED and Swiss Target Prediction in several key points, one of which is the calculation used to predict either the biological activity or binding to a specific target. The second main difference is that each web has a different output. PASS online output is to predict the general biological activity for each metabolite, while Super-PRED explicitly investigates the target prediction of each metabolite on the CYP-450 enzyme. Furthermore, the Swiss Target Prediction provides us with a general prediction for the metabolite binding site. The third significant difference is the database for each web server utilized, as every web server has a unique database to provide us with a holistic view of metabolite activity.

Prediction of Metabolites' Effect on CYP-450 (Super-PRED Web Server)

Based on the concept of comparable characteristics, the Super-PRED Web Server links molecular targets and chemical similarities of drug-like metabolites with treatment approaches. Super-PRED predicts the impact of a metabolite on the body based on the concept that metabolites with similar structures have comparable biological activities.[18]

Metabolites Target Prediction (Swiss Target Prediction Web Server)

Based on the finding that comparable bioactive metabolites are more likely to share similar targets, a Swiss Target Prediction model was created. Thus, the targets of a metabolite can be predicted by selecting proteins with known ligands that are extremely similar to the examined metabolite. In this ligand-based strategy, it is evident that metabolites showing a high degree of similarity in Swiss Target Prediction are more likely to interact with the same target.[19] Additionally, the highest target prediction scored using a score incorporating both 2D and 3D similarity values, with the most comparable known active to the query molecules. Thus, Swiss Target prediction is a major tool for investigating the targets of extracted metabolites.

Table 2 The Reference Range for the Measured Parameters Using the Swiss ADME Web Server

Parameter Name	Lipophilicity: XLOGP3	Size: Molecular Weight	Polarity: TPSA	Solubility: log S	Saturation: Fraction of Carbons in the sp^3 Hybridization	Flexibility
Reference Range	Between −0.7 and +5.0	Between 150 and 500 g/mol	Between 20 and 130 Å^2	Not higher than 6	Not less than 0.25	No more than 9 rotatable bonds

Metabolites' Pharmacokinetics Parameters Prediction (Swiss ADME Web Server)

An effective metabolite must reach its target in the body at a sufficient concentration and remain there in a bioactive state for desired biological activities to occur and be considered an effective medication. The evaluation of absorption, distribution, metabolism, and excretion is a critical step in the drug development process. Using the Swiss ADME Web Server, these ADME characteristics can be assessed separately to modify the metabolite based on the desired therapeutic outcomes.[20] The acceptable ranges of the parameters tested using the Swiss ADME are listed in Table 2.

Organ and Oral Toxicity (ProTox II Web Server)

The ProTox-II Web Server is a freely accessible tool for evaluating the potential toxicity of chemical metabolites and offers a thorough and reliable prediction of different toxicity outcomes.[21] Utilizing various data sources, such as in vitro and in vivo tests, provides a strong and precise forecast of toxicity. Therefore, we used this web server to predict the oral and organ toxicities of the extracted metabolites.

According to Banerjee et al,[22] the ProTox-II Web Server is classified into five different steps: (1) oral toxicity with six classes per LD_{50} value, (2) organ toxicity model for hepatotoxicity prediction, (3) toxicological endpoints with four models, (4) toxicological pathways that involve two major groups of adverse outcome pathways: the nuclear receptor pathway and the stress response pathway with 12 models (seven for nuclear receptors and five for the stress response pathway), and (5) toxicity targets with 15 models, as illustrated in Figure 1.

Cardiac Toxicity (CardioToxCSM Web Server)

Failure to identify major toxicities of drugs, such as cardiovascular toxicity, remains a significant challenge. Web servers, such as the CardioToxCSM Web Server, are convenient tools for predicting cardiotoxicity and minimizing adverse drug effects. The CardioToxCSM Web Server can predict distinct types of cardiac toxicity including arrhythmia, cardiac failure, heart block, hERG toxicity, hypertension, and myocardial infarction.[23] Because the CardioToxCSM Web Server is a helpful and accurate tool for predicting cardiac toxicity, we decided to use it in our study to evaluate metabolites extracted from *B. carteri*.

Molecular Docking Studies (Maestro Software)

Ligand–receptor complex interactions were predicted using molecular docking. This process involves sampling and scoring components as part of the receptor-ligand docking method. Maestro Software was used to perform docking calculations, including prepwizard, ligprep, and grid receptor generation, for the molecular docking investigation of *B. carteri's* metabolites as substrates and both CAR (PDB: 1XVP) and PXR (PDB: 1SKX) as receptors. Each receptor

Class 1:	Fatal if swallowed ($LD_{50} \leq 5$)
Class 2:	Fatal if swallowed ($5 < LD_{50} \leq 50$)
Class 3:	Toxic if swallowed ($50 < LD_{50} \leq 300$)
Class 4:	Harmful if swallowed ($300 < LD_{50} \leq 2000$)
Class 5:	It may be harmful if swallowed ($2000 < LD_{50} \leq 5000$)
Class 6:	Non-toxic ($LD_{50} > 5000$)

Figure 1 Oral toxicity classes per LD_{50} value using Protox-II Web Server.

was docked separately with all identified metabolites of *B. carteri's* identified metabolites as ligands to predict potential molecular interactionsand post-docking analysis was conducted to identify potential agonists.[24]

Human PXR Receptor Competitive Binding Assay

The binding of chemicals from *B. carteri* resin aqueous extracts was determined using the Thermo Scientific LanthaScreen® TR-FRET Pregnane X Receptor Competitive Binding Assay (catalog number PV4839) following the manufacturer's instructions.

Human CAR Coactivator Assay

The binding of chemicals from *B. carteri* resin aqueous extracts was determined using the LanthaScreen™ TR-FRET Constitutive Androstane Receptor Coactivator Assay (catalog number PV4836) following the manufacturer's instructions.

Data Analysis and Statistics

The statistical significance difference of Hep G2 cell treatment with *B. carteri* was calculated using Student's paired *t*-test in relation to untreated control (DMSO-treated) using Excel software. The CYP gene expression results are reported as mean ± standard deviation (SD) and mean ± the standard error of mean (SEM) for the receptor-binding assay results. The results were plotted using the GraphPad (Boston, MA) Prism software (version 5.02).

Results

Our study aimed to elucidate the effects of *B. carteri* on CYP450 enzyme induction. Given the diverse methods of plant preparation employed by consumers, we evaluated sonicated and boiled extracts to simulate the common usage patterns. Our objective was to assess whether these preparation methods differentially influence CYP enzyme activity, potentially leading to clinically significant drugherb interactions. By examining both extraction techniques, we aimed to provide a comprehensive understanding of the effects of *B. carteri's* impact on CYP450-mediated drug metabolism, thereby informing both clinical practice and future pharmacokinetic studies.

Endotoxin and Cytotoxicity

Endotoxin contamination level in the aqueous extracts of *B. carteri* resins was determined using the LAL assay kit, as previously described. The endotoxin contamination level was 14.62 ± 1.146 endotoxin unit (EU)/g *B. carteri* resin, which is acceptable and below the maximum endotoxin contamination level for cell culture. Based on the MTT assay results, we selected three treatment concentrations of 25, 50, and 100 µg/mL for the gene expression experiment using Hep G2 cells. The MTT results revealed no significant cytotoxic effects of aqueous extracts of *B. carteri* resin on Hep G2 cell proliferation at concentrations up to 300.0 µg/mL, as shown in Figure 2.

CYP 1A2, 2B6, and 3A4 Gene Expression by qPCR

The expression of CYP 1A2, 2B6, and 3A4 was determined using RT q-PCR in post-treated Hep G2 cells by *B. carteri* resin aqueous extracts. The analysis revealed that *B. carteri* induced the expression of all three CYP enzymes in a concentration-dependent manner as follows:

For CYP 1A2, all treatment concentrations increased the CYP 1A2 gene expression with an average exceeding 2-fold change at 3.2 ± 1.6, 6.5 ± 4.3, and 9.4 ± 5.4-fold change for sonicated *B. carteri* 25, 50, and 100 µg/mL, respectively, while at 4.7 ± 3.0, 6.3 ± 5.2, and 6.3 ± 2.9-fold change for boiled *B. carteri* 25, 50, and 100 µg/mL, respectively. Rifampicin, the positive inducer control, at a treatment concentration of 1 µM, had an induction effect measure of 2.7 ± 0.8-fold change in comparison to the untreated control, as seen in Figure 3.

For CYP 2B6, all treatment concentrations increased the CYP 2B6 gene expression, with an average exceeding 2-fold change for the highest concentrations at 100 µg/mL. The measured fold-change values were 1.3 ± 0.4, 1.9 ± 0.6, and 3.0 ± 1.0 for sonicated *B. carteri* 25, 50, and 100 µg/mL, respectively, while at 1.5 ± 0.5, 1.8 ± 0.6, and 2.5 ± 1.8 for boiled

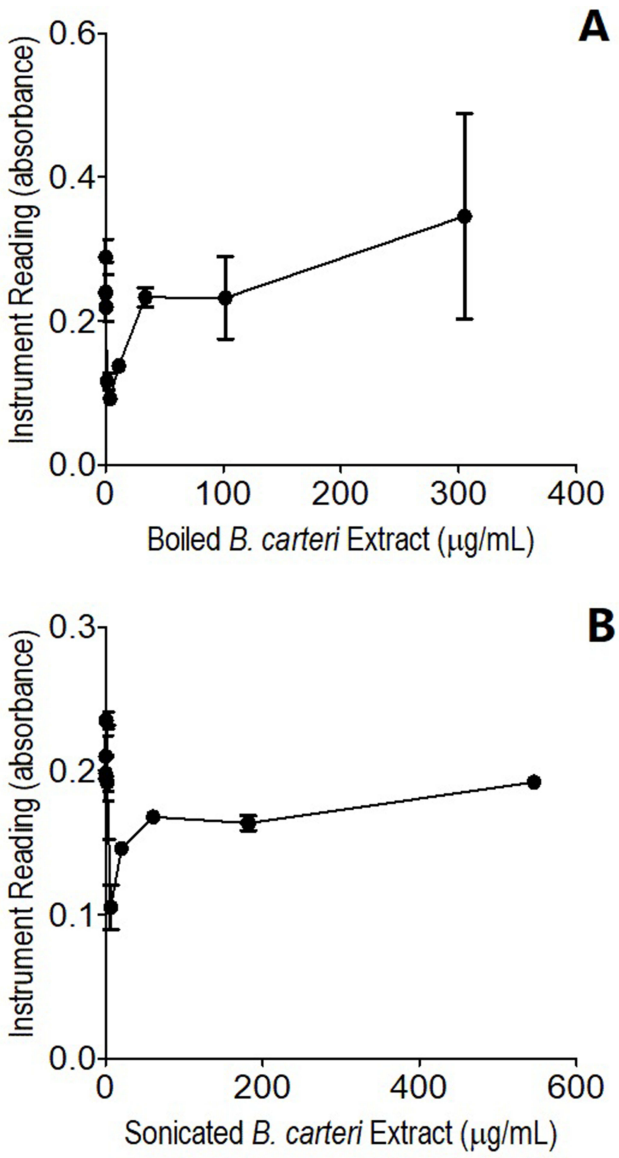

Figure 2 The concentration-proliferation inhibition relationship of the boiled (**A**) and sonicated (**B**) aqueous extracts of *Boswellia carteri* resins on hepatocarcinoma Hep G2 cells. Each point represents mean ± standard deviation from a minimum of three independent experiments.

B. carteri 25, 50, and 100 µg/mL. Rifampicin-induced CYP 2B6 gene expression was measured at a 1.6 ± 0.8-fold change compared to the untreated control, as shown in Figure 3.

For CYP 3A4, all treatment concentrations also increased the CYP 3A4 gene expression, with an average exceeding 2-fold change for the highest concentrations at 100 µg/mL. The measured fold-change values were 1.4 ± 0.2, 1.8 ± 0.3, and 3.2 ± 1.1 for sonicated *B. carteri* 25, 50, and 100 µg/mL, respectively, while at 1.9 ± 0.2, 2.1 ± 1.0, and 2.8 ± 1.0 for boiled *B. carteri* 25, 50, and 100 µg/mL, respectively. Rifampicin-induced CYP 3A4 gene expression was measured at 1.8 ± 1.0-fold change compared to the untreated control, as seen in Figure 3.

Identification of B. carteri Secondary Metabolites Using LC/MS Q-TOF

The crude extract of the *B. carteri* was subjected to total ion current spectra (TIC) raw data, and the data-analysis program Mass Hunter (Agilent Technologies), as well as qualitative and quantitative analysis software was used. The chemical structures of all identified metabolites are shown in Figure 4. After conducting a mass screening on the below spectrum (Figure 5 and Table 3), we have summarized the following: chemical features were extracted from the LC-MS

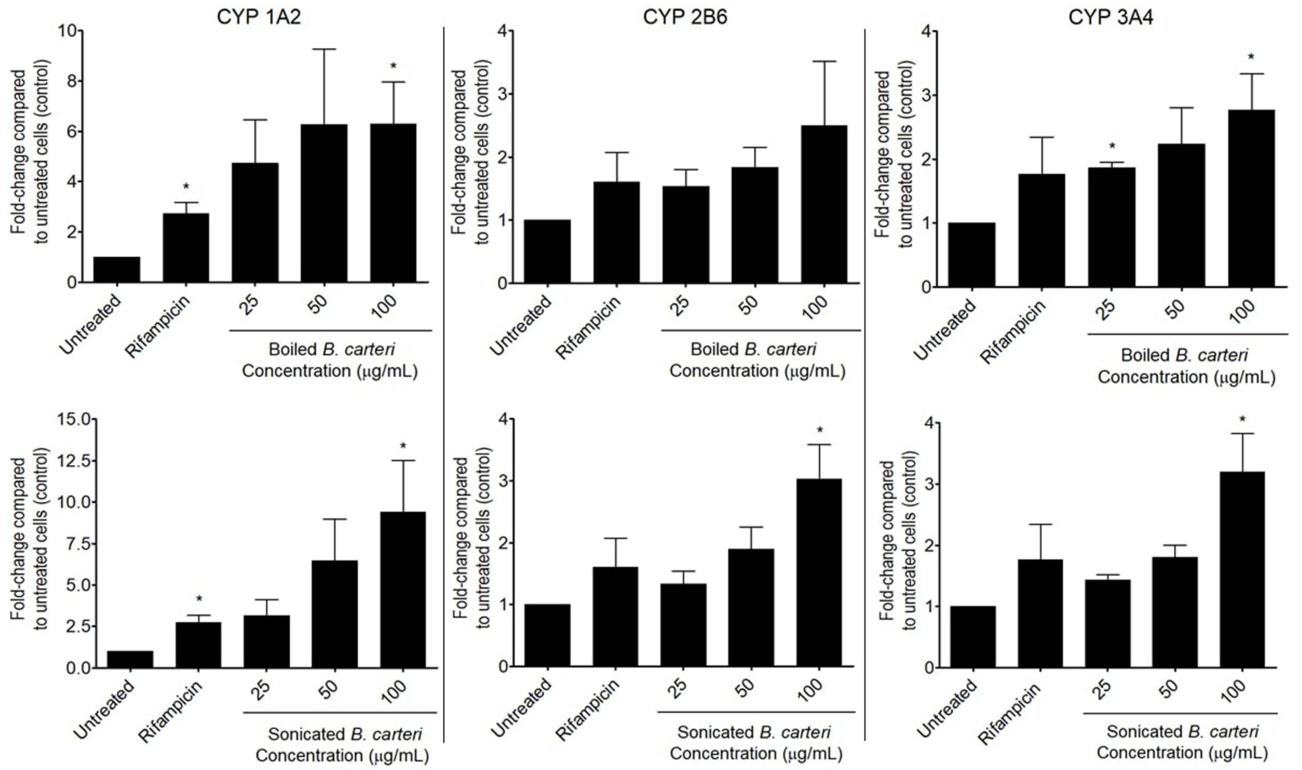

Figure 3 The modulatory effects of boiled and sonicated aqueous extract of *Boswellia carteri* resins on gene expression levels of CYP 1A2 (left), 2B6 (middle), and 3A4 (right) isoenzymes in Hep G2 cells monitored by RT q-PCR. A minimum of three independent cell treatments were performed for each extract concentration. Rifampicin tested at one concentration (1 µM) was used as a positive inducer control. Results are expressed as mean ± SD from a minimum of three independent experiments. Student's *t*-test was used to determine treatment significantly related to untreated control (* $p < 0.05$).

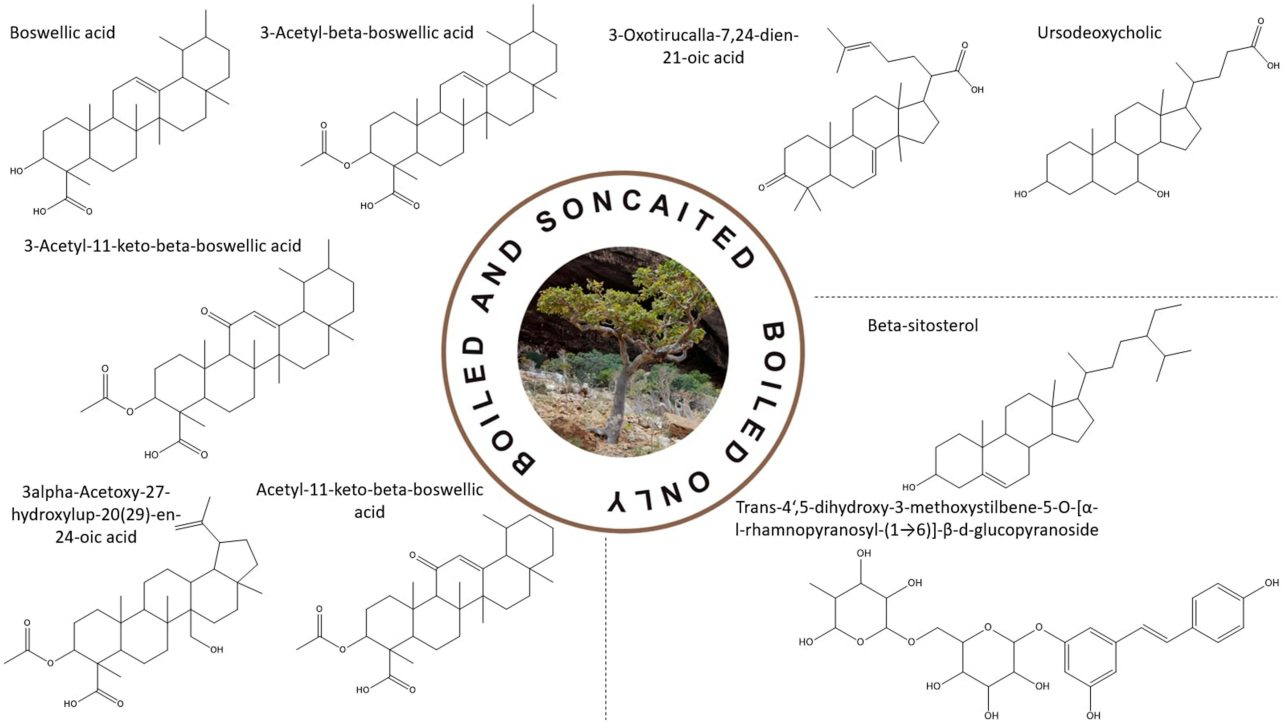

Figure 4 Chemical structures of compounds tentatively identified in *Boswellia carteri* crude extracts prepared via boiling and sonication methods.

https://doi.org/10.2147/BTT.S491278

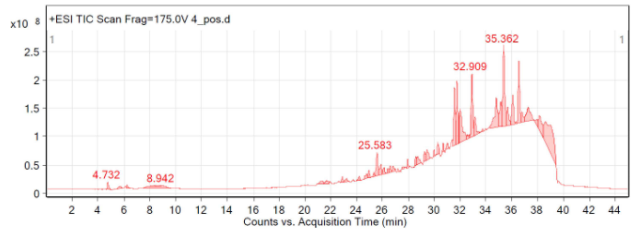

Elector spray ionization total ion chromatogram (Positive Mode) of ***Boswellia carteri*** Boiled Extract

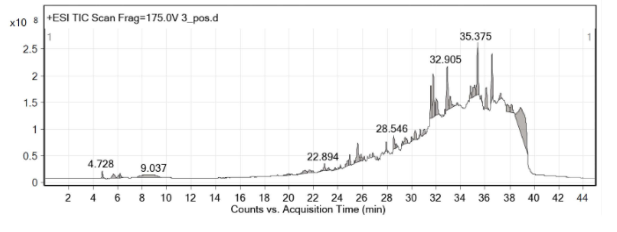

Elector spray ionization total ion chromatogram (Positive Mode) of ***Boswellia carteri*** Sonicated Extract

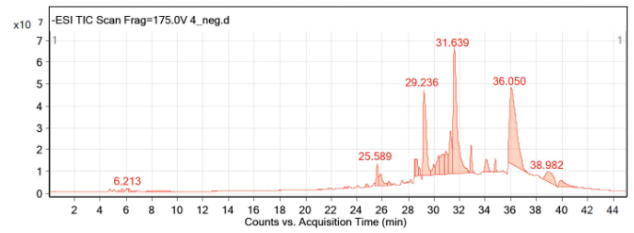

Elector spray ionization total ion chromatogram (Negative Mode) of ***Boswellia carteri*** Boiled Extract

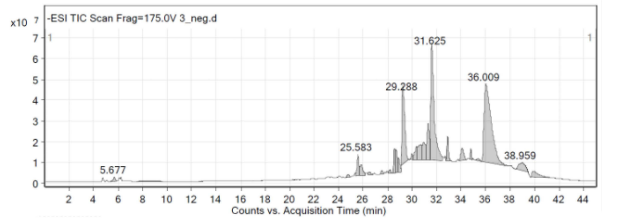

Elector spray ionization total ion chromatogram (Negative Mode) of ***Boswellia carteri*** Sonicated Extract

Figure 5 Electrospray ionization total ion chromatogram (positive and negative mode) of *Boswellia carteri* (boiled and sonicated) extracts.

data using the Molecular Features Extraction (MFE) algorithm and recursive analysis workflow. Features were extracted by screening the detected nodes at various retention times per minute, with a minimum intensity of 6000 counts, and were aligned with previously detected metabolites considering adducts ($[M^+K]^+$ and $[M^-H]^-$). Boswellic acid, according to Wang et al,[25] 3-Acetyl-beta-boswellic acid, according to Wang et al,[25] 3alpha-Acetoxy-27-hydroxylup-20(29)-en-24-

Table 3 Metabolites (M1–M9) Tentatively Identified from Boswellia Carteri Boiled and Sonicated Aqueous Extracts

Peak No.	Rt (min)	$[M^+H]^+$	$[M^-H]^-$	Err PPM	Molecular Formula	Tentative Identification	Extraction Method	Literature Review of the Metabolites
Peak A (M1)	(35.578–35.876)	458.3	455.7	− 0.95	$C_{30}H_{48}O_3$	Boswellic acid	Boiled, and Sonicated Extracts	(Wang, F., Li, Z. L., et el, 2011)
Peak B (M2)	(35.578–35.876)	499.3	497.6	−0.80	$C_{32}H_{50}O_4$	3-Acetyl-beta-boswellic acid	Boiled, and Sonicated Extracts	(Wang, F., Li, Z. L., et el, 2011)
Peak C (M3)	(38.395–39.406)	515.6	513.6	−0.45	$C_{32}H_{50}O_5$	3alpha-Acetoxy-27-hydroxylup-20(29)-en-24-oic acid	Boiled, and Sonicated Extracts	Ammon, H. P. T. (2010).
Peak D (M4)	(38.395–39.406)	513.6	511.7	−0.65	$C_{32}H_{48}O_5$	3-Acetyl-11-keto-beta-boswellic acid	Boiled, and Sonicated Extracts	Ammon, H. P. T. (2010).
Peak E (M5)	(25.450–25.517)	455.6	453.9	−0.45	$C_{30}H_{46}O_3$	3-Oxotirucalla-7,24-dien-21-oic acid	Boiled, and Sonicated Extracts	(Wang, F., Li, Z. L., et el, 2011)
Peak F (M6)	(29.484–29.650)	393.6	391.8	−0.65	$C_{24}H_{40}O_4$	Ursodeoxycholic acid	Boiled, and Sonicated Extracts	(Nani, et el, 2009)
Peak G (M7)	(25.754–25.821)	537.6	535.5	− 0.80	$C_{26}H_{32}O_{12}$	trans-4',5-dihydroxy-3-methoxystilbene-5-O-[α-l-rhamnopyranosyl-(1→6)]-β-d-glucopyranoside	Boiled Extract only	(Atta-ur-Rahman, et al, 2005)

(*Continued*)

Table 3 (Continued).

Peak No.	Rt (min)	$[M^+H]^+$	$[M^-H]^-$	Err PPM	Molecular Formula	Tentative Identification	Extraction Method	Literature Review of the Metabolites
Peak H (M8)	(28.604–28.868)	417.7	415.8	− 0.70	$C_{29}H_{50}O$	B-Sitosterol	Boiled Extract only	(Atta-ur-Rahman, et al, 2005)
Peak I (M9)	(22.020–22.467)	513.5	511.8	−0.65	$C_{32}H_{48}O_5$	Acetyl-11-keto-beta-boswellic acid	Boiled, and Sonicated Extracts	(Mannino, G., et al, 2016)

oic acid, according to Ammon HPT,2010,[26] 3-Acetyl-11-keto-beta-boswellic acid, according to Ammon HPT,2010.[26] 3-Oxotirucalla-7,24-dien-21-oic acid, according to Wang et al,[25] Ursodeoxycholic acid, according to Yang et al,[27] trans-4',5-dihydroxy-3-methoxystilbene-5-O-[α-l-rhamnopyranosyl-(1→6)]-β-d-glucopyranoside, according to Attaur Rahman et al[28] beta-Sitosterol, according to Attaur Rahman et al.[28] Acetyl-11-keto-beta-boswellic acid, according to Mannino G,[29] means *m/z* implies measured *m/z*.

In silico Studies

The primary objective of this study was to evaluate CYP450 enzyme induction mediated by *B. carteri* extracts. Using both the boiled and sonicated extraction methods, we identified seven common metabolites across both techniques. Furthermore, two additional metabolites, which were trans-4',5-dihydroxy-3-methoxystilbene-5-O-[α-L-rhamnopyranosyl-(1→6)]-β-D-glucopyranoside and beta-sitosterol were exclusively detected in the boiled extract. After metabolite identification, we employed in silico methodologies to elucidate the pharmacokinetic properties, potential molecular targets, and biological activities of the metabolites. This computational approach aimed to comprehensively characterize the bioactive constituents of *B. carteri's* bioactive constituents and their potential interactions with CYP enzymes, thereby offering insights into the possible mechanisms of enzyme induction.

PASS Web Server

The PASS Web Server was used to computationally predict the probability of biological activity for each metabolite based on its structure by comparing it with previously reported biologically active substrates in the database. The primary findings of this study were P_a (probable activity) and P_i (probable inactivity). Metabolites with P_a values greater than P_i are considered potential candidates for biological activity.[30] The values obtained for the extracted metabolites were based on the probable activity. If the bioactivity score is greater than 0.70 ($P_a > 0.70$), the predicted pharmacological activities would have a high probability of being experimentally observed. As this is the focus of this study, we investigated the metabolites that could act as inducers or substrates of CYP isoenzymes. The activities of other predicted metabolites are summarized in Supplemental Tables S1–S9. Only five identified metabolites, 3-Oxotirucalla 7.24-dien-21-oic acid, Boswellic acid, Ursodeoxych olic acid, Trans-4',5 dihydroxy-3 methoxystilbene-5-O- [α-l rhamnopyranosyl-(1→6)], β-d-glucopyranoside, and beta-sitosterol show potential action on CYP enzymes, as listed in Table 4.

Table 4 Metabolites of Boswellia Carteri Plant Possessing CYP Enzyme Activity and Their Activity (P_a) and Inactivity (P_i) Probabilities Using PASS Online Web Server

Metabolite Name	Biological Activity	Probability of Activity (P_a)	Probability of Inactivity (P_i)
3-Oxotirucalla-7,24-dien-21-oic acid	CYP2J substrate	0.821	0.016
Boswellic Acid	CYP2J substrate	0.713	0.046

(*Continued*)

https://doi.org/10.2147/BTT.S491278

Table 4 (Continued).

Metabolite Name	Biological Activity	Probability of Activity (P_a)	Probability of Inactivity (P_i)
Ursodeoxych olic acid	CYP4B substrate	0.956	0.001
	CYP4B1 substrate	0.953	0.001
	CYP4A11 substrate	0.931	0.001
	CYP2C substrate	0.928	0.004
	CYP2B6 substrate	0.917	0.003
	CYP2J substrate	0.898	0.005
	CYP2J2 substrate	0.889	0.004
	CYP3A4 substrate	0.885	0.007
	CYP3A4 inducer	0.869	0.004
	CYP3A substrate	0.870	0.008
	CYP3A inducer	0.849	0.004
	CYP3A2 substrate	0.822	0.004
	CYP2C19 substrate	0.814	0.004
	CYP2C11 substrate	0.777	0.004
	CYP2C9 inducer	0.760	0.003
	CYP2B substrate	0.749	0.009
	CYP3A5 substrate	0.743	0.011
	CYP4A substrate	0.714	0.003
	CYP3A1 substrate	0.713	0.009
Trans-4',5-dihydroxy-3-methoxystilbene-5-O-[α-l-rhamnopyranosyl-(1→6)]-β-d-glucopyranoside	CYP2H substrate	0.789	0.019

(*Continued*)

Table 4 (Continued).

Metabolite Name	Biological Activity	Probability of Activity (P_a)	Probability of Inactivity (P_i)
Beta-Sitosterol	CYP2C substrate	0.909	0.005
	CYP3A4 substrate	0.882	0.007
	CYP4B substrate	0.869	0.001
	CYP3A4 inducer	0.868	0.004
	CYP3A inducer	0.866	0.004
	CYP4B1 substrate	0.859	0.001
	CYP3A substrate	0.865	0.008
	CYP2C11 substrate	0.848	0.003
	CYP2J substrate	0.824	0.015
	CYP3A5 substrate	0.801	0.006
	CYP2J2 substrate	0.800	0.013
	CYP2C19 substrate	0.744	0.005
	CYP2C12 substrate	0.753	0.047

Super-PRED Web Server

The Super-PRED Web Server was used to investigate potential therapeutic targets for metabolites extracted from the *B. carteri* plant using boiling and sonication methods. Based on the Super-PRED server, the most probable targets for every analyzed metabolite had a probability of ≥80%.[31] As a result, nine extracted metabolites' targets (probability >90%) were predicted and are listed in conjunction with their Swiss Target Prediction in Table 5. The metabolites listed in the Super-PRED section of the table are presented as predicted data. Notably, none of the nine metabolites indicated experimental data, except for beta-sitosterol, which was reported to act via the tyrosyl-DNA phosphodiesterase one enzyme with PDB visualization (PDB ID: 6N0D).[32]

Swiss Target Prediction Web Server

The Swiss Target Prediction Web Server is an online tool that helps accurately estimate the macromolecular targets of small metabolites assumed to be bioactive. Using SMILEs as inputs, the website provides a prediction based on a combination of 2D and 3D similarities with known ligands.[19] In our study, we used Swiss Target Prediction to estimate molecular targets. Furthermore, we selected the top 15 predictions for each extracted metabolite, and the results are shown in a chart representing the potential molecular targets, as detailed in Table 5 and Figure 6. 3-Acetyl-11 keto-beta

https://doi.org/10.2147/BTT.S491278

Table 5 Molecular Target Prediction for Extracted Metabolites from Boswellia Carteri Plant Using Super-PRED

Metabolite Name	Target Prediction (Super-PERD)		
	Target Name	Probability (%)	PDB Visualization
3-Acetyl-11 keto-beta boswellic acid	11-beta-hydroxysteroid dehydrogenase 2	96.46%	Not Available
	11-beta-hydroxysteroid dehydrogenase 2	96.46%	Not Available
	Dual specificity protein kinase CLK4	92.73%	6FYV
	Dual specificity protein kinase CLK4	92.73%	6FYV
	Cathepsin D	92.08%	4OD9
	Signal transducer and activator of transcription 3	90.85%	6QHD
	Cytochrome P450 3A4	90.53%	5VCC
3-Acetyl beta boswellic acid	Nuclear factor NF-kappa-B p105 subunit	97.25%	1SVC
	Dual specificity protein kinase CLK4	90.75%	6FYV
3-Oxotirucalla 7.24-dien-21-oic acid	DNA (apurinic or apyrimidinic site) lyase	96.14%	6BOW
	Cyclooxygenase-1	94.89%	6Y3C
	Nuclear factor NF-kappa-B p105 subunit	94.68%	1SVC
	MAP kinase ERK2	93.08%	6SLG
	Cathepsin D	92.72%	4OD9
	G-protein coupled receptor 55	90.14%	Not Available
3alpha-acetoxy-27-hydroxylup-20(29)-en-24-oic acid	Nuclear factor NF-kappa-B p105 subunit	98.07%	1SVC
	Dual specificity protein kinase CLK4	95.34%	6FYV
	Mu opioid receptor	93.09%	Not Available
	Cannabinoid CB2 receptor	91.56%	6KPF
	Cannabinoid CB1 receptor	90.83%	6N4B
	Dihydroorotate dehydrogenase	90.24%	6FMD
	Cytochrome P450 3A4	90.13%	5VCC
Boswellic acid	Cyclooxygenase-1	96.03%	6Y3C
	Nuclear factor NF-kappa-B p105 subunit	91.59%	1SVC
	G-protein coupled receptor 55	91.44%	Not Available
Acetyl-11 keto-beta-boswellic acid	11-beta-hydroxysteroid dehydrogenase 2	96.46%	Not Available
	Nuclear factor NF-kappa-B p105 subunit	96.42%	1SVC
	Dual specificity protein kinase CLK4	92.73%	6FYV
	Cathepsin D	92.08%	4OD9
	Signal transducer and activator of transcription 3	90.85%	6QHD
	Cytochrome P450 3A4	90.53%	5VCC

(*Continued*)

Table 5 (Continued).

Metabolite Name	Target Prediction (Super-PERD)		
	Target Name	Probability (%)	PDB Visualization
Ursodeoxycholic acid	Cyclooxygenase-1	98.88%	6Y3C
	Nuclear factor NF-kappa-B p105 subunit	97.84%	1SVC
	Cannabinoid CB2 receptor	95.86%	6KPF
	Kappa opioid receptor	92.55%	4DJH
	Acetylcholines terase	92.44%	1F8U
	Beta-glucocerebrosidase	92.11%	6TN1
Trans-4',5-dihydroxy-3-methoxystilbene-5-O-[α-l-rhamnopyranosyl-(1→6)]-β-d-glucopyranoside	DNA- (apurinic or apyrimidinic site) lyase	99.02%	6BOW
	Adenosine A1 receptor	95.31%	5N25
	Pregnane X receptor	95.05%	6TFI
	Kruppel-like factor 5	93.67%	NA
	Estrogen receptor beta	91.34%	1QKM
	15-hydroxyprostaglandin dehydrogenase [NAD^+]	91.29%	2GDZ
	Nuclear factor NF-kappa-B p105 subunit	91.02%	1SVC
	Cathepsin D	90.9%	4OD9
	Nuclear factor erythroid 2-related factor 2	90.6%	2FLU
Beta-Sitosterol	Nuclear factor NF-kappa-B p105 subunit	97%	1SVC
	Cathepsin D	96%	4OD9
	Adenosine A1 receptor	94%	5N2S
	Cannabinoid CB2 receptor	94%	6KPF
	Dual specificity protein kinase CLK4	92.7%	6FYV
	Cyclooxygenase-1	92%	6Y3C
	Mineralocorticoid receptor	91%	4PF3
	Glutamate NMDA receptor; GRIN1/GRIN2B	90%	5EWM
	G-protein coupled receptor 55	90%	Not Available
Beta-Sitosterol	Tyrosyl-DNA phosphodiesterase 1		6N0D

boswellic acid, 3-Acetyl beta boswellic acid, 3-Oxotirucalla 7.24-dien-21-oic acid, Acetyl-11 keto-beta-boswellic acid, Boswellic acid, 3alpha-acetoxy-27-hydroxylup-20(29)-en-24-oic acid, and Ursodeoxycholic acid had enzyme as their highest target prediction with or without specification regarding which enzyme they are targeting. Meanwhile, the other metabolites had nuclear receptors, proteases, oxidoreductase, and Family A G-protein as their main target predictions.

Swiss ADME Web Server

It is crucial to investigate the pharmacokinetic properties of the metabolites extracted from *B. carteri* plant. The importance of this investigation is to characterize the metabolites' properties as hydrophilicity, hydrogen bond acceptors,

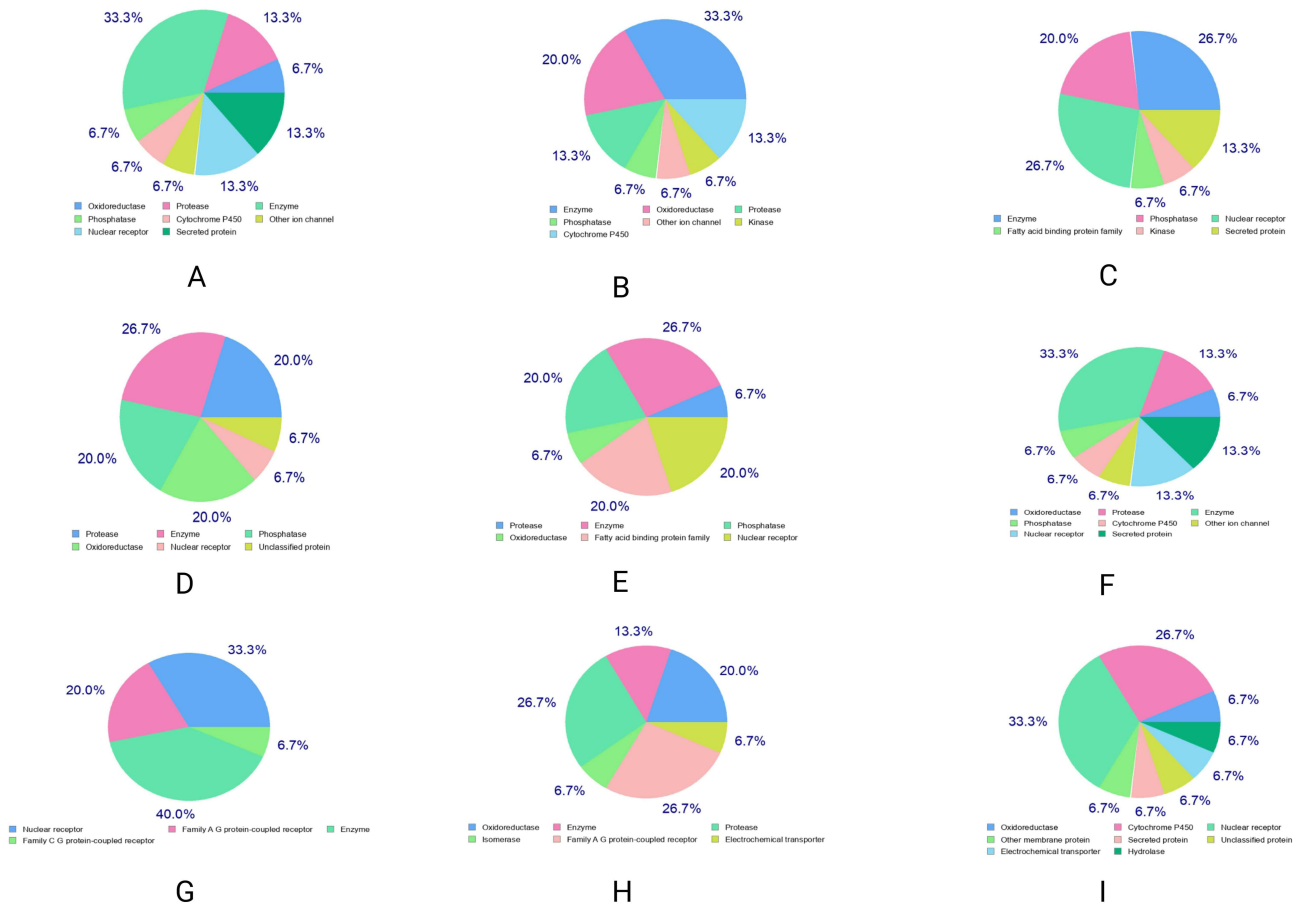

Figure 6 Molecular target prediction for extracted metabolites from *Boswellia carteri* plant using Swiss Target prediction webserver. The predictions from lift to right are: (**A**) 3-Acetyl-11-keto-beta-boswellic acid, (**B**) 3-Acetyl-beta-boswellic acid, (**C**) 3-Oxotirucalla-7,24-dien-21-oic acid, (**D**) 3alpha-Acetoxy-27-hydroxylup-20(29)-en-24-oic acid, (**E**) Boswellic Acid, (**F**) Acetyl-11-keto-beta-boswellic acid, (**G**) Ursodeoxycholic acid, (**H**) Trans-4',5-dihydroxy-3-methoxystilbene-5-O-[α-l-rhamnopyranosyl-(1→6)]-β-d-glucopyranoside, (**I**) Beta-sitosterol.

and donors, which play a key role in predicting how the metabolite will interact with bodily means, such as phospholipid membranes and the blood–brain barrier. Additionally, pharmacokinetic properties help to determine the potential drug-herbal interactions between the metabolites extracted from *B. carteri* plant and other substances used as medications. As a result, we performed Swiss ADME to illustrate the effect of *B. carteri* plant's extracted metabolites and their pharmacokinetic properties to discover potential drug-herbal interaction in the pharmacokinetic aspect.

Six physicochemical properties were investigated for each identified metabolite, including lipophilicity, size, polarity, solubility, flexibility, and saturation, using the bioavailability radar from the Swiss ADME Web Server, which is essential for determining Lipinski's rule of five. Lipinski's rule of five is known as a metabolite with the following characteristics: a molecular mass of less than 500 Da, a maximum of five hydrogen bond donors, a maximum of 10 hydrogen bond acceptors, and a log P value for the octanol-water partition coefficient that is not greater than 5. Lipinski's rule of five is considered a guideline for predicting the degree of metabolite's absorption. Furthermore, Lipinski's rule of five assesses the drug-likeness of a chemical metaboliteand whether a chemical metabolite exhibits certain pharmacological or biological activity that is likely to render its absorption.[31]

Based on the Swiss ADME analysis, of the nine *B. carteri*'s metabolites, only one metabolite, ursodeoxycholic acid, followed Lipinski's rule without a single violation. However, the remaining metabolites violated Lipinski's rule. The additional results from the Swiss ADME are presented in Table 6 and Figure 7.

Table 6 Results of Boswellia Carteri 'S Metabolites Using Swiss ADME Web Server

Metabolite Name	Lipophilicity: XLOGP3	Size: Molecular Weight	Polarity: TPSA	Solubility: log S	Saturation: Fraction of Carbons in the sp^3 Hybridization	Flexibility
3-Acetyl-11 keto-beta boswellic acid	7.22	512.72 g/mol	0.67 Å²	−7.37	0.84	3
3-Acetyl beta boswellic acid	8.29	498.74 g/mol	63.60 Å²	−7.96	0.88	3
3-Oxotirucalla 7.24-dien-21-oic acid	7.45	454.68 g/mol	54.37 Å²	−7.02	0.80	5
3alpha-acetoxy-27-hydroxylup-20(29)-en-24-oic acid	7.74	514.74 g/mol	83.83 Å²	−7.58	0.88	5
Boswellic acid	8.26	456.70 g/mol	57.53 Å²	−7.81	0.90	1
Acetyl-11 keto-beta-boswellic acid	7.22	512.72 g/mol	80.67 Å²	−7.37	0.84	3
Ursodeoxycholic acid	3.08	392.57 g/mol	77.76 Å²	−3.95	0.96	4
Trans-4',5-dihydroxy-3-methoxystilbene-5-O-[α-l-rhamnopyranosyl-(1→6)]-β-d-glucopyranoside	0.13	536.53 g/mol	198.76 Å²	−3.95	0.46	7
Beta-Sitosterol	9.34	414.71 g/mol	20.23 Å²	−7.90	0.93	6

Protox-II Web Server

One of the most important aspects in the development of new drugs is safety, which includes the assessment of potential toxicities. Currently, animal trials are the primary means for evaluating the toxic effects of drug candidates and cosmetics. However, in silico prediction methods offer an alternative avenue.

In our study, we focused on both oral and organ toxicity as they play a significant role in drug safety. After uploading the SMILEs of our metabolites, the output showed the toxicity class, predicted median lethal dose (LD_{50}) in mg/kg body weight, average similarity in percentage, and predicted accuracy with metabolites that had the most identical oral toxicity values compared to the studied rodent oral toxicity values from the database, as shown in Table 7.[33] Refer to Figure 1 for oral toxicity classification based on LD_{50}.

Almost all the metabolites may be orally harmful (Class V) per the LD_{50} value and require a larger dose to exert harm compared with the other lower classes. Boswellic Acid metabolite is shown to be non-toxic (Class VI). Moreover, Beta-sitosterol, Ursodeoxycholic acid, and 3-Oxotirucalla-7,24-dien-21-oic acid were classified as harmful after swallowing (Class IV), as shown in Table 7.

The predicted toxicity model report of the input metabolite is shown, if available, with the classification, target name, average fit, and similarity to the pharmacophore and well-known ligands of the respective targets. The prediction of organ toxicity, specifically hepatotoxicity, carcinogenicity, mutagenicity, and immunotoxicity, is presented, along with their probabilities. Among the metabolites investigated, 8 out of 9 are non-hepatotoxic, including 3-Acetyl-11-keto-beta-boswellic acid, 3-Acetyl-beta-boswellic acid, 3-Oxotirucalla-7,24-dien-21-oic acid, 3alpha-Acetoxy-27-hydroxylup-20(29)-en-24-oic acid, Boswellic Acid, Acetyl-11-keto-beta-boswellic acid, trans-4',5-dihydroxy-3-methoxystilbene-5-O-[α-l-rhamnopyranosyl-(1→6)]-β-d-glucopyranoside, and Beta-sitosterol, with probability value ranging from 0.53 to 0.87. In contrast, the only metabolite showing active hepatotoxicity was Ursodeoxycholic acid, with a probability value of 0.73. With regard to carcinogenicity, all metabolites except 3alpha-Acetoxy-27-hydroxylup-20(29)-en-24-oic acid, Ursodeoxycholic acid, trans-4',5-dihydroxy-3-methoxystilbene-5-O-[α-l-rhamnopyranosyl-(1→6)]-β-d-glucopyranoside, and Beta-sitosterol were classified as active carcinogens, with a probability value of 0.54 and 0.55. Furthermore, Ursodeoxycholic acid was the only metabolite with inactive immunotoxicity with a probability value of 0.78. Finally, all the metabolites were inactive in terms of mutagenicity, as illustrated in Table 8.

CardioToxCSM Web Server

After uploading the SMILEs of our metabolites, the output showed different types of cardiotoxicities, such as arrhythmia, cardiac failure, heart block, hERG toxicity, hypertension, and myocardial infarction. All of the metabolites had 3 out of 6 cardiotoxicity types. Regarding arrhythmia, 3-Acetyl-11-keto-beta-boswellic acid, 3-Acetyl-beta-boswellic acid, 3alpha-

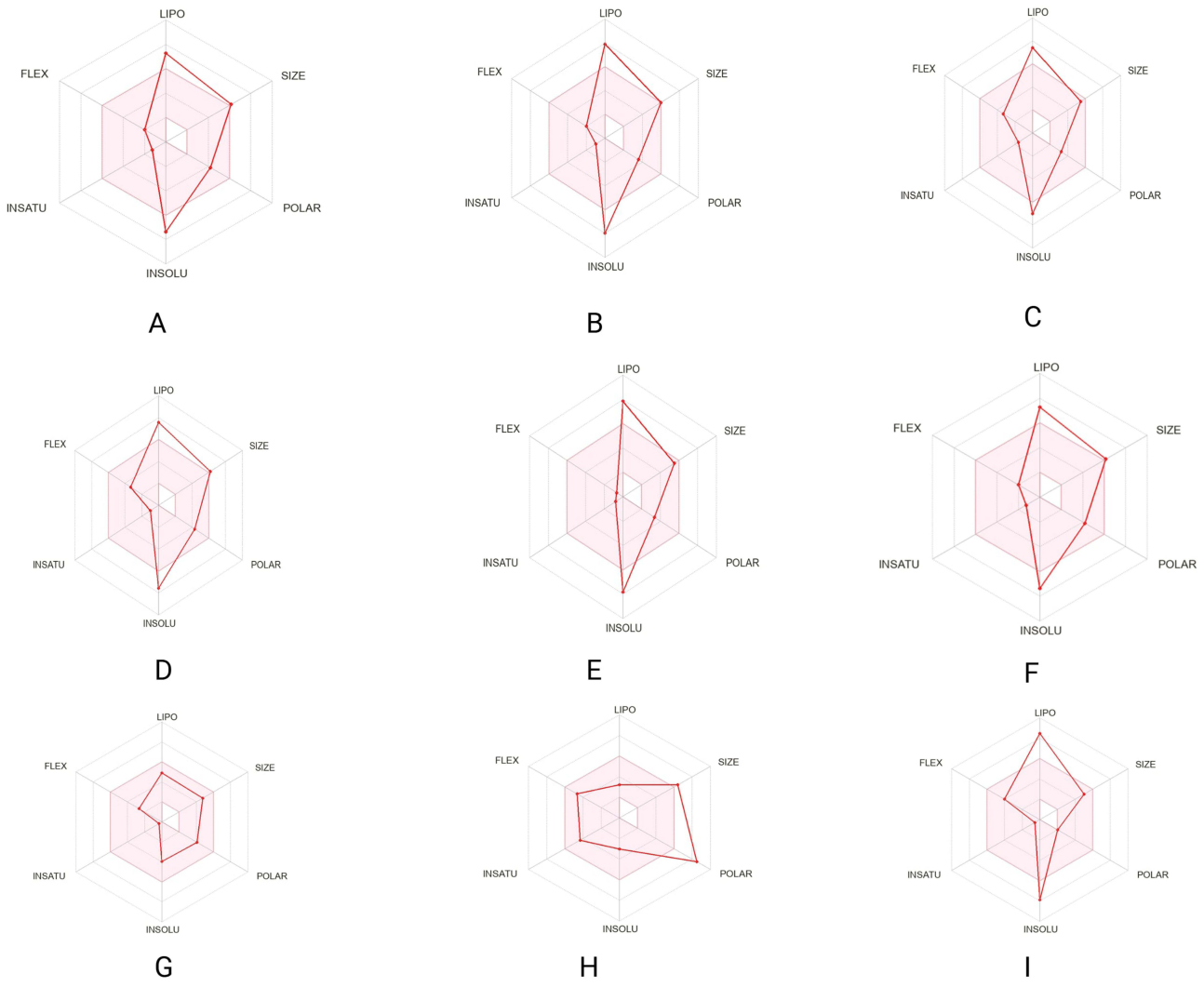

Figure 7 Results of *Boswellia carteri* 's metabolites using Swiss ADME Web Server. The predictions from lift to right are: (**A**) 3-Acetyl-11-keto-beta-boswellic acid, (**B**) 3-Acetyl-beta-boswellic acid, (**C**) 3-Oxotirucalla-7,24-dien-21-oic acid, (**D**) 3alpha-Acetoxy-27-hydroxylup-20(29)-en-24-oic acid, (**E**) Boswellic Acid, (**F**) Acetyl-11-keto-beta -boswellic acid, (**G**) Ursodeoxycholic acid, (**H**) Trans-4',5-dihydroxy-3-methoxystilbene-5-O-[α-l-rhamnopyranosyl-(1→6)]-β-d-glucopyranoside, (**I**) Beta-sitosterol.

Acetoxy-27-hydroxylup-20(29)-en-24-oic acid, Boswellic Acid, Acetyl-11-keto-beta-boswellic acid, and Beta-sitosterol showed positive results. Moreover, cardiac failure is predicted for 3-Oxotirucalla-7,24-dien-21-oic acid, Ursodeoxycholic acid, and Trans-4',5-dihydroxy-3-methoxystilbene-5-O-[α-l-rhamnopyranosyl-(1→6)]-β-d-glucopyranosid. None of the metabolites exhibited heart blockade or hERG toxicity. Finally, all metabolites showed positive results for hypertension and myocardial infarction, as shown in Table 9.

Table 7 Oral Toxicity Prediction of Boswellia Carteri Plant Metabolites Using Protox-II Web Server

Metabolite Name	Predicted LD_{50} in mg/kg Body Weight	Predicted Toxicity Class	Average Similarity	Predicted Accuracy
3-Acetyl-11-keto-beta-boswellic acid	3300	V	84.75%	70.97%
3-Acetyl-beta-boswellic acid	3300	V	77.75%	69.26%

(*Continued*)

Table 7 (Continued).

Metabolite Name	Predicted LD_{50} in mg/kg Body Weight	Predicted Toxicity Class	Average Similarity	Predicted Accuracy
3-Oxotirucalla-7,24-dien-21-oic acid	1000	IV	87.39%	70.97%
3alpha-Acetoxy-27-hydroxylup-20(29)-en-24-oic acid	5000	V	75.85%	69.26%
Boswellic Acid	11800	VI	88.57%	70.97%
Acetyl-11-keto-beta-boswellic acid	3300	V	84.75%	70.97%
Ursodeoxycholic acid	2000	IV	100%	100%
Trans-4',5-dihydroxy-3-methoxystilbene-5-O-[α-l-rhamnopyranosyl-(1→6)]-β-d-glucopyranoside	3750	V	68%	68.07%
Beta-sitosterol	890	IV	89.38%	70.97%

Molecular Docking

Molecular interaction and docking studies are crucial for elucidating the binding mechanisms between metabolites extracted from *B. carteri's* and CYP enzymes, specifically focusing on PXR and CAR. These interactions are hypothesized to be the potential mediators of CYP enzyme induction.

Table 8 Organ Toxicity Profiles of Boswellia Carteri's Extracted Metabolites Using Protox-II Web Server

Metabolite Name	Organ Toxicity/ Toxicity Endpoints	Probability	Prediction
3-Acetyl-11-keto-beta-boswellic acid	Hepatotoxicity	0.76	Inactive
	Carcinogenicity	0.54	Active
	Immunotoxicity	0.99	Active
	Mutagenicity	0.95	Inactive
3-Acetyl-beta-boswellic acid	Hepatotoxicity	0.76	Inactive
	Carcinogenicity	0.54	Active
	Immunotoxicity	0.97	Active
	Mutagenicity	0.95	Inactive
3-Oxotirucalla-7,24-dien-21-oic acid	Hepatotoxicity	0.77	Inactive
	Carcinogenicity	0.55	Active
	Immunotoxicity	0.63	Active
	Mutagenicity	0.94	Inactive
3alpha-Acetoxy-27-hydroxylup-20(29)-en-24-oic acid	Hepatotoxicity	0.86	Inactive
	Carcinogenicity	0.69	Inactive
	Immunotoxicity	0.80	Active
	Mutagenicity	0.77	Inactive

(*Continued*)

https://doi.org/10.2147/BTT.S491278

Table 8 (Continued).

Metabolite Name	Organ Toxicity/ Toxicity Endpoints	Probability	Prediction
Boswellic Acid	Hepatotoxicity	0.53	Inactive
	Carcinogenicity	0.55	Active
	Immunotoxicity	0.93	Active
	Mutagenicity	0.88	Inactive
Acetyl-11-keto-beta-boswellic acid	Hepatotoxicity	0.76	Inactive
	Carcinogenicity	0.54	Active
	Immunotoxicity	0.99	Active
	Mutagenicity	0.95	Inactive
Ursodeoxycholic acid	Hepatotoxicity	0.73	Active
	Carcinogenicity	0.79	Inactive
	Immunotoxicity	0.78	Inactive
	Mutagenicity	0.56	Inactive
Trans-4',5-dihydroxy-3-methoxystilbene-5-O-[α-l-rhamnopyranosyl-(1→6)]-β-d-glucopyranoside	Hepatotoxicity	0.80	Inactive
	Carcinogenicity	0.85	Inactive
	Immunotoxicity	0.99	Active
	Mutagenicity	0.77	Inactive
Beta-sitosterol	Hepatotoxicity	0.87	Inactive
	Carcinogenicity	0.60	Inactive
	Immunotoxicity	0.99	Active
	Mutagenicity	0.98	Inactive

Table 9 Predicted Cardiac Toxicity of Boswellia Carteri's Extracted Metabolites Using CardioToxCSM Web Server

Metabolite Name	Arrhythmia	Cardiac Failure	Heart Block	hERG Toxicity	Hypertension	Myocardial infarction
3-Acetyl-11-keto-beta-boswellic acid	1	0	0	0	1	1
3-Acetyl-beta-boswellic acid	1	0	0	0	1	1
3-Oxotirucalla-7,24-dien-21-oic acid	0	1	0	0	1	1
3alpha-Acetoxy-27-hydroxylup-20(29)-en-24-oic acid	1	0	0	0	1	1
Boswellic Acid	1	0	0	0	1	1
Acetyl-11-keto-beta-boswellic acid	1	0	0	0	1	1
Ursodeoxycholic acid	0	1	0	0	1	1
Trans-4',5-dihydroxy-3-methoxystilbene-5-O-[α-l-rhamnopyranosyl-(1→6)]-β-d-glucopyranosid	0	1	0	0	1	1
Beta-sitosterol	1	0	0	0	1	1

Notes: 0 = cardiosafe metabolite, 1 = cardiotoxic metabolite.

In silico docking studies were performed using the PXR receptor, with Rifampicin serving as a positive control for ligand binding. Among the analyzed metabolites, only trans-4',5-dihydroxy-3-methoxystilbene-5-O-[α-L-rhamnopyranosyl-(1→6)]-β-D-glucopyranoside exhibited hydrogen bonding interactions with Serine 247, Lysine 210, and Glycine 285 residues of the PXR binding pocket. In addition, Boswellic acid exhibited hydrogen bonding with Glycine 285 residues.

A quantitative assessment of binding affinities was conducted using docking score analysis, and the results are presented in Table 10.

Three-dimensional representations of the docked complexes are illustrated in Figure 8, providing visual insights into the spatial orientation and interactions of ligands within the receptor-binding site.

A molecular docking study was performed on the CAR receptor using the metabolites extracted from *B. carteri*. 6-(4-Chlorophenyl) imidazo[2,1-b][1,3]thiazole-5-carbaldehyde O-(3,4-dichlorobenzyl)oxime (CITCO), a potent and selective CAR agonist, was employed as a positive control to establish a reference for ligand-binding affinity with Pi-pi stacking bonds with Phenylalanine 217 residue.

Among the docked metabolites, β-Sitosterol and Ursodeoxycholic acid demonstrated notable interactions within the CAR-binding pocket. Specifically, β-Sitosterol formed a hydrogen bond with the Asparagine 165 residue, while Ursodeoxycholic acid exhibited hydrogen bonding with the Valine 199 residue. These interactions suggest the potential modulatory effects on CAR activity.

A quantitative assessment of the docking study was conducted, and the results are presented in Table 11.

Three-dimensional representations of the docked complexes are illustrated in Figure 9, providing spatial insights into ligand orientation and interactions within the CAR-binding site. The docking scores and structural visualizations collectively offer a comprehensive evaluation of the potential CAR-mediated effects of *B. carteri* metabolites.

Nuclear Receptors PXR and CAR Binding

For the PXR competitive binding assay, both the boiled and sonicated *B. carteri* aqueous extracts showed no display of ligand binding, while Rifampicin, the PXR agonist ligand control, had an IC_{50} value of approximately 0.39 ± 0.28 μM, as seen in Figure 10. In contrast, both boiled and sonicated *B. carteri* aqueous extracts displayed agonist mode slopes for the CAR, as seen in Figure 11. The half-maximal effective concentration (EC_{50}) values for boiled and sonicated *B. carteri* are 7.9 ± 5.1 and 222.6 ± 198.1 μg/mL, respectively. The CAR agonist control of CITCO had an EC_{50} value measured at 0.48 ± 0.22 nM.

Discussion

According to estimates from the World Health Organization, 80% of the global population uses natural health products, particularly herbal medicines, as first-line therapy.[34] Numerous studies in many countries have reported a high prevalence of herbal medicine use in patients. For example, approximately 29% of 217 Turkish patients with chronic diseases were reported to consume herbal medicines.[35] In the United Kingdom, one study reported that approximately 20% of 1134 patients with cancer use herbal medicines.[36] In Japan, approximately 31% of 1321 patients with rheumatoid arthritis use dietary supplements and/or herbal medicines.[37] In China, 53% of 587 cancer patients use herbal medicines without

Table 10 Docking Scores of Boswellia Carteri's Metabolites and PXR Receptor

Metabolite Name	Docking Score (PXR receptor)	Molecular Interactions
Rifampicin (Native ligand)	−11.012	H-bonds with (HIS 407 and GLN 285) Salt bridge with ARG 410
Trans-4',5-dihydroxy-3-methoxystilbene-5-O-[α-l-rhamnopyranosyl-(1→6)]-β-d-glucopyranoside	−9.368	H-bonds with (LYS 210, SER247, and GLN 285)
Boswellic acid	−8.252	H-bond with GLN 285

https://doi.org/10.2147/BTT.S491278

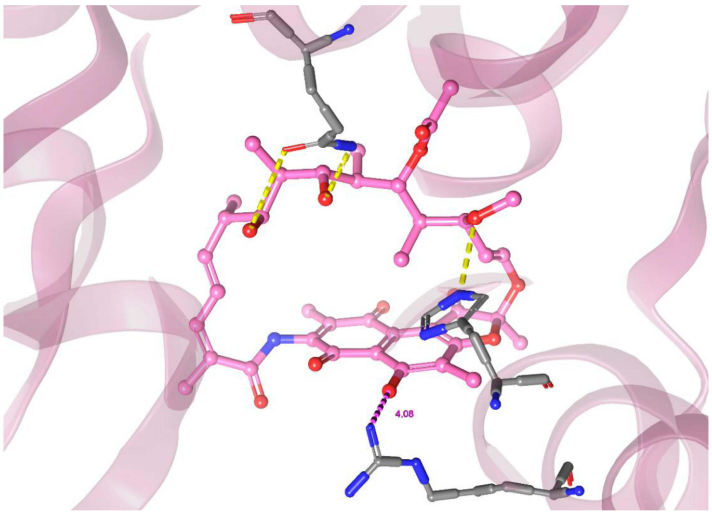

A) Rifampicin (native ligand)

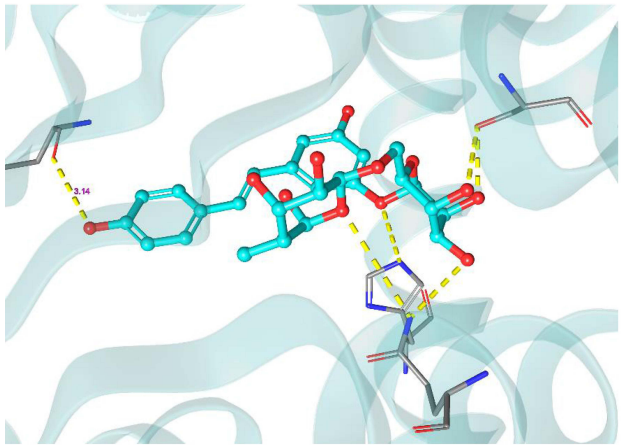

B) Trans-4‘,5-dihydroxy-3-methoxystilbene-5

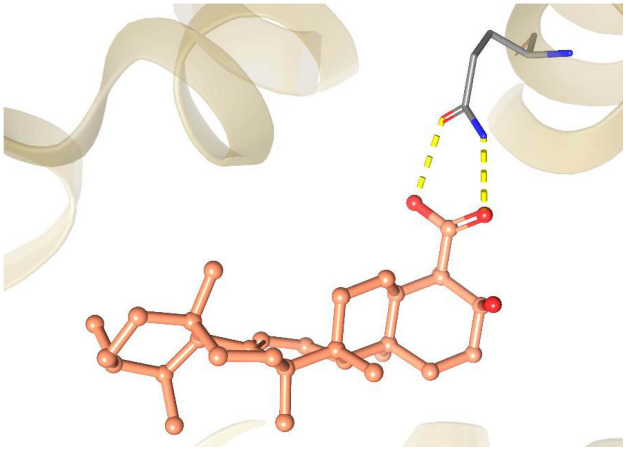

C) Boswellic acid

Figure 8 Three-dimensional molecular docking visualization of PXR receptor in complex with rifampicin and selected metabolites extracted from *Boswellia carteri*. The ligands are represented as follows: (**A**) Rifampicin (positive control): faded magenta, (**B**) Boswellic acid: faded azure, (**C**) Trans-4',5-dihydroxy-3-methoxystilbene-5-O-[α-L-rhamnopyranosyl-(1→6)]-β-D-glucopyranoside: faded Orange. Hydrogen bonds between the ligands and PXR residues are shown as yellow dashed lines, and salt bridge is purple.

consulting practitioners.[38] In Saudi Arabia, the prevalence of herbal medicine use among patients is higher. One study found that 77% of 200 patients use herbal medicines with minimal medical supervision.[39] Another study reported that 68% of 235 patients with chronic diseases use herbal medicines without medical supervision.[40] Thus, studies of CYP-mediated drug interactions are crucial and highly needed as previous studies have reported that many herbal medicines

Table 11 Docking Scores of Boswellia Carteri's Metabolites and CAR Receptor

Metabolite Name	Docking Score (CAR receptor)	Molecular Interactions
CITCO (native ligand)	−10.862	Pi-pi stacking (PHE 217)
β-Sitosterol	−11.104	H-bond (ASN 165)
Ursodeoxycholic acid	−10.856	H-bond (VAL 199)

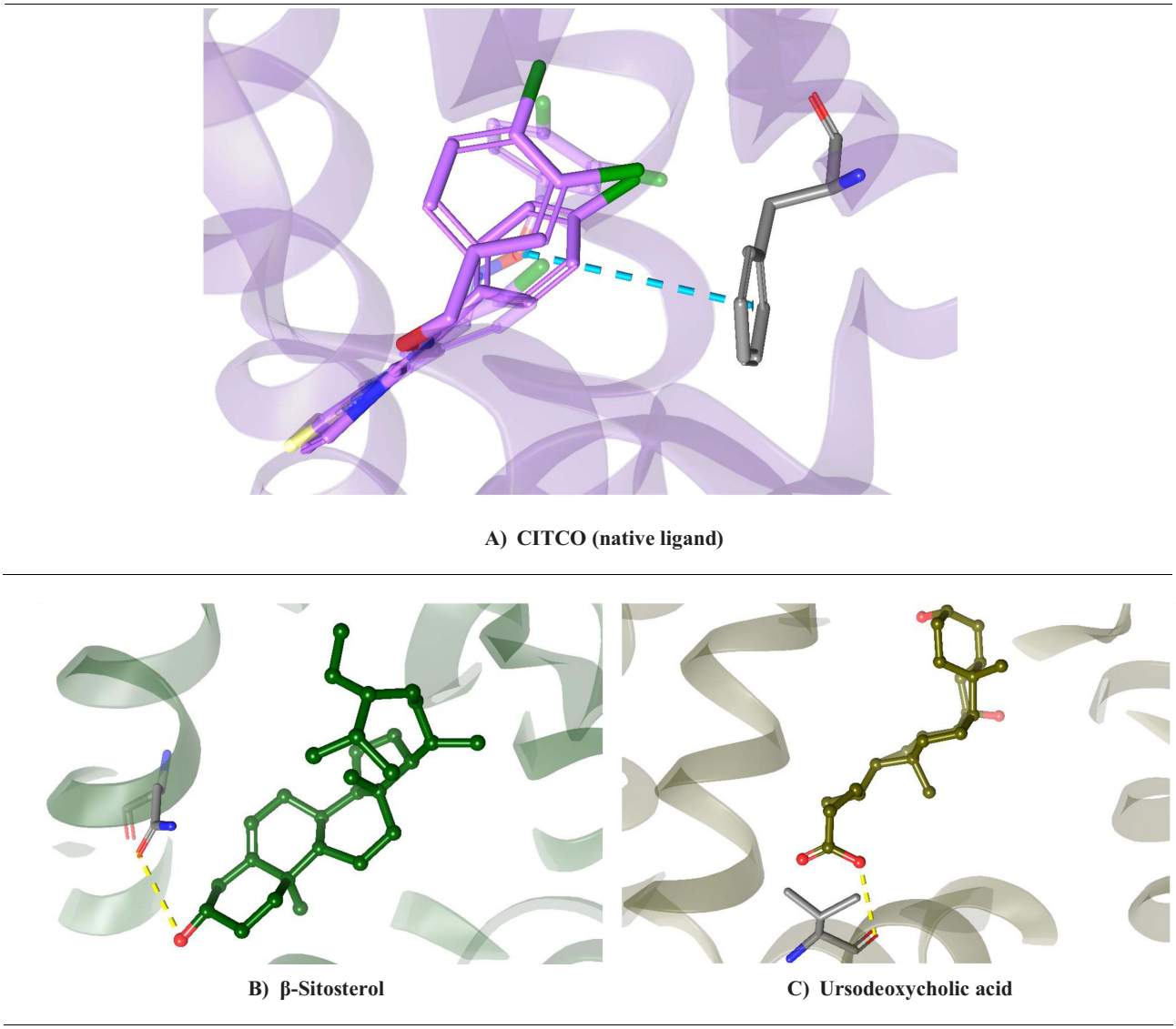

Figure 9 Three-dimensional molecular docking visualization of CAR receptor in complex with CITCO and selected metabolites extracted from *Boswellia carteri*. The ligands are represented as stick models and color-coded as follows: (**A**) CITCO (6-(4-Chlorophenyl) imidazo[2,1-b][1,3]thiazole-5-carbaldehyde O-(3,4-dichlorobenzyl)oxime; positive control): Purple, (**B**) β-Sitosterol: Green, (**C**) Ursodeoxycholic acid: dark gold. Hydrogen bonds between the ligands and CAR residues are shown as yellow dashed lines, and pi-pi stacking is light blue.

are strong inhibitors or inducers of CYP isoenzymes. An example is the "grapefruit effect" where flavonoids and coumarins, mainly naringin, bergamottin, and 6.7-dihydroxybergamottin, from the grapefruit strongly inhibit intestinal CYP 3A4.[41] On the other hand, the popular St. John's Wort, an herbal medicine used for the treatment of depression, menopausal symptoms, and attention-deficit hyperactivity disorder, contains hyperforin which is reported to be a strong inducer of CYP 3A4 activity via PXR activation.[42]

In this study, we performed several in vitro and in silico studies to confirm the modulatory effects of the popular resins from *B. carteri* on three important CYP enzyme gene expressions.

Endotoxin, Cytotoxicity and CYP Enzyme Gene Expression Measurement

Initially, the *B. carteri* resins were extracted twice using sonication and boiling to mimic the traditional methods of maceration and decoction preparations, respectively, as different preparation temperatures might result in different modulations of CYP enzyme expression by the resin extracts due to different phytochemical compositions. After

https://doi.org/10.2147/BTT.S491278

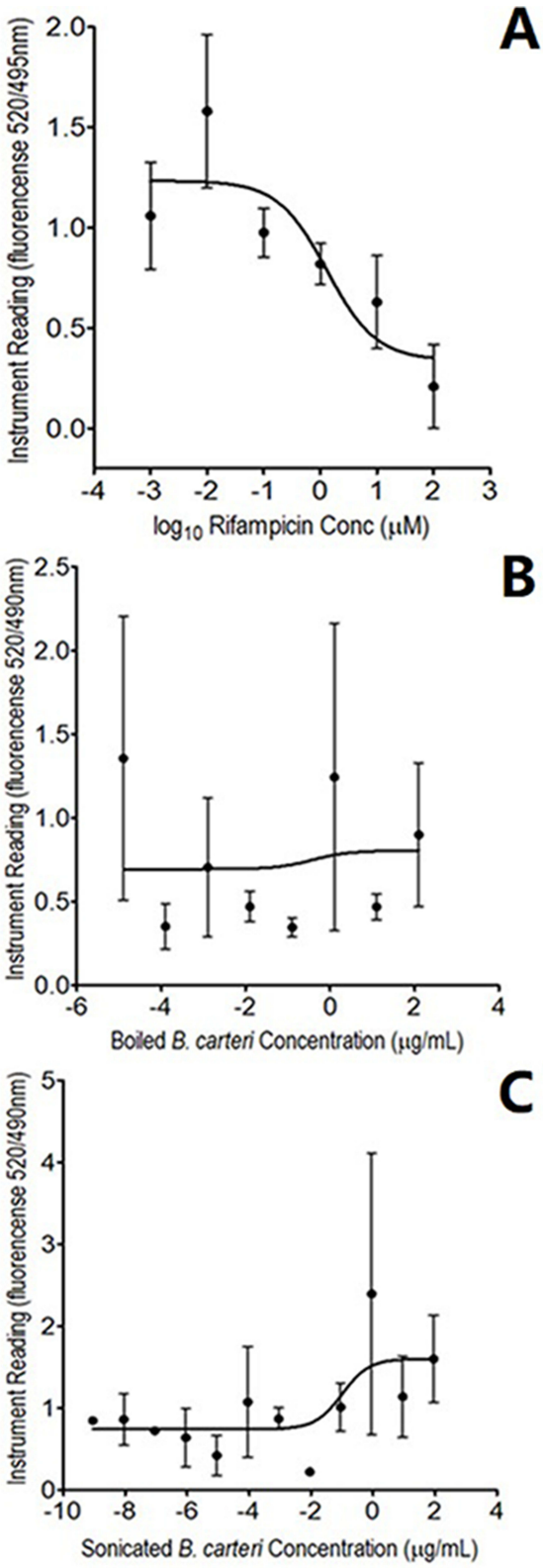

Figure 10 The concentration-inhibition of rifampicin (**A**), *Boswellia carteri* resins boiled (**B**), and sonicated (**C**) aqueous extracts in the LanthaScreen® TR-FRET PXR Competitive Binding Assay. The dots stand for mean ± standard error of the mean (SEM) from a minimum of three independent experiments.

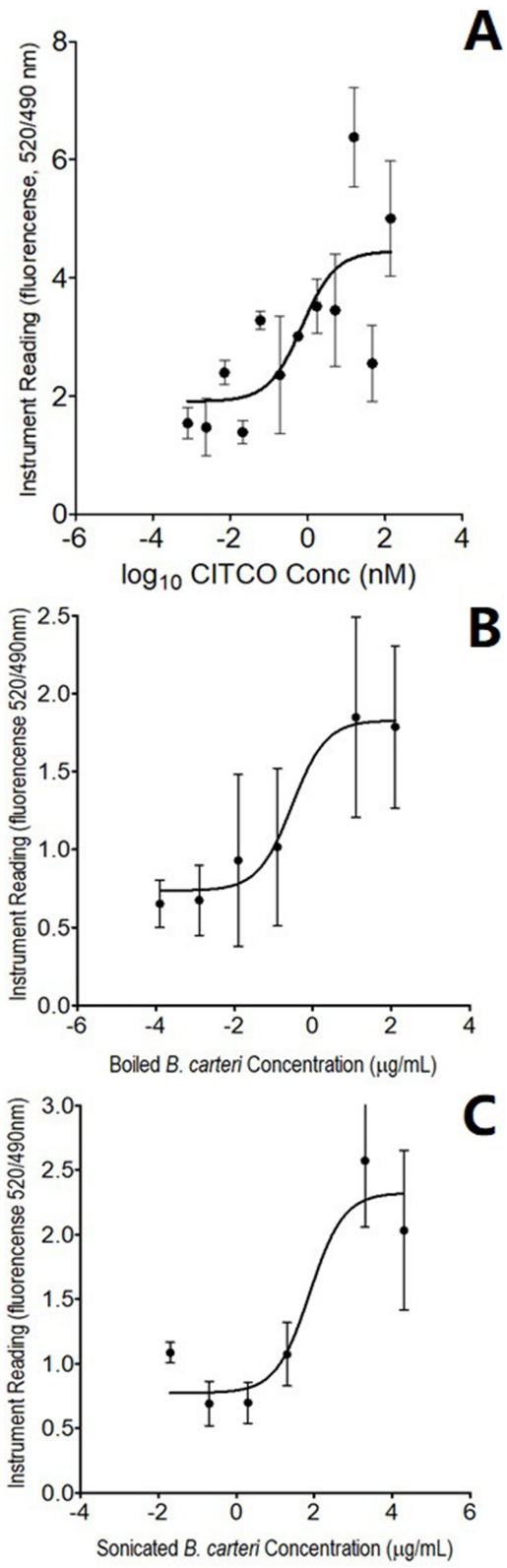

Figure 11 The concentration-inhibition of CITCO (**A**), *Boswellia carteri* resins boiled (**B**) and sonicated (**C**) aqueous extracts in the LanthaScreen® TR-FRET CAR Coactivator Assay. The dots represent mean ± SE from a minimum of three independent experiments.

https://doi.org/10.2147/BTT.S491278

which, the endotoxin contamination levels in both aqueous extracts of *B. carteri* were measured and the levels were determined to be lower than the maximum reported endotoxin contamination level of 1×10^4 EU/mL for cell culture.[43] Thus, endotoxin removal step for *B. carteri* aqueous extracts prior to Hep G2 cell treatment was unnecessary. Notably, elevated endotoxin contamination levels are reported to interfere with CYP enzyme expression in cell culture, which justifies the endotoxin contamination measurement in this study.[44] Next, we determined the antiproliferative effect of boiled and sonicated aqueous extracts of *B. carteri* resins on Hep G2 cells according to the United States Food and Drug Administration (USFDA) Guidelines for Industry – In Vitro Drug Interaction Studies Cytochrome P450 Enzyme – and Transporter-Mediated Drug Interactions. In this study, we selected the Hep G2 cells to conduct CYP induction experiments as these cells are widely used in the CYP induction detection studies and contain a higher basal level of CYP enzymes in comparison to related cell lines.[45,46] Cytotoxicity was determined using the MTT assay and revealed no significant cytotoxic effect at higher *B. carteri* extract concentrations, as mentioned earlier. It should be noted that cytotoxic concentration treatments can influence (ie, decrease) gene expression levels of CYP enzymes in cultured cells.[47] As per the USFDA guidelines, we measured the induction effect of *B. carteri* on three main CYP enzymes, including 1A2, 2B6, and 3A4, as recommended. These three enzymes represent the three major regulators of CYP enzymes: AhR, CAR, and PXR, respectively.[48] In this study, we determined the modulatory effect of *B. carteri* on CYP enzymes by measuring the mRNA levels of the three CYP enzymes as an alternative to the CYP-specific drug probe substrate biotransformation rate measurement, which can be interfered with enzyme inhibitors from the phytochemical mixture.[48] The remaining study design elements of this CYP induction study were aligned with USFDA guideline recommendations.

In this study, Rifampicin was selected as a positive inducer control for CYP 3A4 as per the recommendations of the USFDA guidelines. Rifampicin increased the average mRNA levels of the CYP 3A4 enzyme by more than 1.5-fold compared to the untreated control, which is close to the typical fold-change reported by the USFDA guidelines for Rifampicin at a 2-fold change increase.[48] Although Rifampicin is not the preferred in vitro inducer drug for studies related to CYP 2B6, a noticeable increase in CYP 2B6 mRNA levels was observed, which is consistent with previous reports that Rifampicin induces CYP 2B6 enzyme levels.[49,50] Furthermore, Rifampicin was not preferred as a CYP 1A2 inducer control; however, we noticed an increase in CYP 1A2 mRNA levels after pretreatment of Hep G2 cells with Rifampicin. Notably, Rifampicin was found to be an in vivo inducer for CYP 1A2 enzyme activity in earlier published studies.[51,52] RT-qPCR results revealed that the average induction levels of CYP 1A2, 2B6, and 3A4 exceed the 2-fold change level set by the USFDA guidelines as a positive induction effect. Based on USFDA guidelines, the aqueous extracts of *B. carteri* are considered inducers of the aforementioned CYP enzymes and most likely for the remaining main CYP enzymes, including CYP 2C enzymes, as they share the same metabolic regulatory pathways.[48]

Tentative Identification of B. carteri Secondary Metabolites

Peak A (M1) the *m/z* value that was visible during the retention period (35.578–35.876) with $[M^+H]^+$ *m/z* in positive mode 458.3 with $[M^-H]^-$ *m/z* in negative mode 455.7. Daltons and a molecular formula of C30H48O3 the *m/z* value that was discernible throughout retention Boswellic acid,[25] the metabolite is tentatively identified in the boiled and sonicated aqueous extracts.

Peak B (M2) the *m/z* value that was visible during the retention period (35.578–35.876) with $[M^+H]^+$ *m/z* in positive mode 499.3 with $[M^-H]^-$ *m/z* in negative mode 497.6. Daltons and a molecular formula of C32H50O4 the *m/z* value that was discernible throughout retention 3-Acetyl-beta-boswellic acid,[25] The metabolite is tentatively identified in the boiled and sonicated aqueous extracts.

Peak C (M3) the *m/z* value that was visible during the retention period (38.395–39.406) with $[M^+H]^+$ *m/z* in positive mode 515.6 with $[M^-H]^-$ *m/z* in negative mode 513.6. Daltons and a molecular formula of C32H50O5 the *m/z* value that was discernible throughout the retention of 3alpha-Acetoxy-27-hydroxylup-20(29)-en-24-oic acid.[26] The metabolite was tentatively identified in the boiled and sonicated aqueous extracts.

Peak D (M4) the m/z value that was visible during the retention period (38.395–39.406) with $[M^+H]^+$ *m/z* in positive mode 513.6 with $[M^-H]^-$ *m/z* in negative mode 511.7. Daltons and molecular formula of C32H48O5 the *m/z* value that

was discernible throughout the retention of 3-Acetyl-11-keto-beta-boswellic acid.[26] The metabolite was tentatively identified in the boiled and sonicated aqueous extracts.

Peak E (M5) the *m/z* value that was visible during the retention period (25.450–25.517) with $[M^{+}H]^{+}$ *m/z* in positive mode 455.6 with $[M^{-}H]^{-}$ *m/z* in negative mode 453.9. Daltons and molecular formula of C30H46O3 were correlated with the parent metabolite 3-Oxotirucalla-7,24-dien-21-oic acid.[25] The metabolite was tentatively identified in the boiled and sonicated aqueous extracts.

Peak F (M6) the *m/z* value that was visible during the retention period (29.484–29.650) with $[M^{+}H]^{+}$ *m/z* in positive mode 393.6 with $[M^{-}H]^{-}$ *m/z* in negative mode 391.8. Daltons and molecular formula of C24H40O4 the *m/z* value was discernible throughout the retention Ursodeoxycholic acid.[27] The metabolite was tentatively identified in the boiled and sonicated aqueous extracts.

Peak G (M7) the *m/z* value that was visible during the retention period (25.754–25.821) with $[M^{+}H]^{+}$ *m/z* in positive mode 537.6 with $[M^{-}H]^{-}$ *m/z* in negative mode 535.5. Daltons and molecular formula of C26H32O12 the *m/z* value that was discernible throughout retention trans-4',5-dihydroxy-3-methoxystilbene-5-O-[α-l-rhamnopyranosyl-(1→6)]-β-d--glucopyranoside.[28] Metabolites were tentatively identified only in the boiled aqueous extract.

Peak H (M8) the *m/z* value that was visible during the retention period (28.604–28.868) with $[M^{+}H]^{+}$ *m/z* in positive mode 417.7 with $[M^{-}H]^{-}$ *m/z* in negative mode 415.8. Daltons and molecular formula of C29H50O the *m/z* value was discernible throughout the retention of beta-sitosterol.[28] Metabolites were tentatively identified only in the boiled aqueous extract.

Peak I (M9) the *m/z* value that was visible during the retention period (22.020–22.467) with $[M^{+}H]^{+}$ *m/z* in positive mode 513.5 with $[M^{-}H]^{-}$ *m/z* in negative mode 511.8. Daltons and a molecular formula of C32H48O5 the m*/z* value that was discernible throughout the retention of Acetyl-11-keto-beta-boswellic acid.[29] The metabolite was tentatively identified in the boiled and sonicated aqueous extracts.

Prediction of B. carteri Metabolites' Biological Effect via PASS Online Web Server

The prediction of *B. carteri* effect on CYP enzymes remains unclear. Following investigation of the biological outcome by the PASS online web server, it was revealed that out of all *B. carteri's* metabolites, only 3-Oxotirucalla-7,24-dien-21-oic acid, trans-4',5-dihydroxy-3-methoxystilbene-5-O-[α-l-rhamnopyranosyl-(1→6)] β-d-glucopyranoside, beta-sitosterol, ursodeoxycholic acid, and boswellic acid show potential biological effect for CYP. Based on ursodeoxycholic acid—adverse effects and drug interaction studies, the ursodeoxycholic acid metabolite shows CYP induction.[53] Moreover, ursodeoxycholic acid showed the highest probability of having a biological effect on CYP compared to the other extracted metabolites.

Prediction of the CYP Activity Using Super-Pred Web Server

As a study aimed to investigate the potential anti-inflammatory and scar-healing properties of Mongolian horse oil, Super-Pred was used to locate the targets of interest, and the Super-Pred Web Server was used to determine *B. carteri's* metabolites' CYP activity.[18] With the notable exception of beta-sitosterol, which targets the tyrosyl-DNA phosphodiesterase 1 enzyme, and a PDB image of 6N0D, none of the metabolites provided experimental evidence.[54] In addition to the previous information, beta-sitosterol is a substrate for CYP, which was confirmed using the Pass Online Web Server. Interestingly, beta-sitosterol showed nine predicted data with several targets, such as the G-protein-coupled receptor and mineralocorticoid receptor, with probabilities equal to 90% and 91%, respectively.

Prediction for the B. carteri Metabolites' Molecular Targets by Swiss Target Prediction

Using a ligand-based strategy, it is evident that metabolites showing a high degree of similarity, as predicted by Swiss Target Prediction, are likely to interact with similar targets.[19,24] All the metabolites target enzymes, which could include the CYP enzyme. 3-Acetyl-11 keto-beta boswellic acid, 3-Acetyl beta boswellic acid, Acetyl-11 keto-beta-boswellic acid, and beta-sitosterol directly interacted with CYP-450 enzymes. At the same time, the other metabolites showed high enzyme prediction as their main target without directly binding to CYP-450 as the main target, which could indicate that the four metabolites mentioned earlier have an impact on CYP-450.

Prediction of B. carteri Metabolites' Pharmacokinetics by Swiss ADME Web Server

In one study, the bark extract of *Rhizophora mucronata* was associated with a protective effect against liver cell line toxicity from a variety of toxicants.[55] Using Swiss ADME eases their study as Swiss ADME online server provides them with predictions regarding the pharmacokinetic impact of the detected metabolites on the inhibition of the CYP enzyme.[20] We predicted the *B. carteri* pharmacokinetic properties using Swiss ADME. Pharmacokinetics plays a significant role in CYP enzyme binding. Of the metabolites of *B. carteri*, only one metabolite, ursodeoxycholic acid, complied with Lipinski's rule according to the Swiss ADME investigation. As ursodeoxycholic acid complies with Lipinski's rule and demonstrates the highest likelihood of having a biological effect on CYP by analysis using the PASS online web server, it may be a metabolite that induces CYP.

As ursodeoxycholic acid complies with Lipinski's rule and demonstrates the highest likelihood of having a biological effect on CYP by analysis using the PASS online web server, it may be a metabolite that induces CYP as it showed favorable pharmacokinetic properties and produces a biological impact on CYP enzyme. Ultimately, this prediction tool (Swiss ADME web server) could improve the pharmacokinetic prediction, helping us to investigate which metabolite is responsible for CYP-450 enzyme induction.

Oral and Organ Toxicity Using Protox-II Web Server

The mechanism of oral toxicity indicated that eight metabolites were classified as class IV and V (harmful and may be harmful if swallowed), whereas one metabolite was classified as class II (death after swallowing).[22] These results suggest that most of the metabolites are relatively safe from the perspective of oral toxicity. Moreover, the organ toxicity profile of *B. carteri* was assessed, revealing that all metabolites were non-hepatotoxic, except for (Ursodeoxycholic acid). In addition, we studied carcinogenicity, immunotoxicity, and mutagenicity. Almost all metabolites exhibited immunotoxicity and carcinogenicity, whereas none of the metabolites exhibited mutagenicity. The literature lacks similar studies regarding organ toxicity induced by *B. carteri*, which makes our study unique. These findings could help to prevent future herb-induced toxicity.

Cardiotoxicity Prediction Using CardioToxCMS Web Server

The CardioToxCMS Web Server identifies cardiac toxicity related to arrhythmia, cardiac failure, heart block, hERG toxicity, hypertension, and myocardial infarction. In a systematic review, *B. carteri* extracts were shown to have antioxidant and anti-inflammatory effects. These effects are the underlying mechanisms of the cardioprotective effects of 3-O-acetyl-11-keto-β-boswellic acid and 3-O-Acetyl-11-keto-β-boswellic acid.[56] Moreover, the literature lacks studies that have identified the cardiac toxicity of *B. carteri* using the CardioToxCMS Web Server.

Docking of B. carteri Metabolites' Using Maestro Software

Post-docking studies of the extracted metabolites of *B. carteri* significantly improved the metabolite targeting prediction for each extracted metabolite. A lower docking score is indicative of better binding affinity to the receptors, which are the PXR and CAR receptors. Four metabolites showed additional hydrogen bonding to the protein residues in the binding site, which showed stronger binding to the active site compared to other metabolites. For docking of extracted metabolites against the CAR receptor, we used CITCO as a reference for the bonding of the extracted metabolites. Only β-Sitosterol and Ursodeoxycholic acid showed docking scores comparable to those of CITCO. Additionally, Ursodeoxycholic acid had a lower docking score than β-Sitosterol, indicating a higher affinity for the CAR receptor and even higher affinity than CITCO. Both β-Sitosterol and Ursodeoxycholic acid exhibit one hydrogen binding, as CITCO has different protein residues in the binding site and a different type of bond (Pi-pi stacking bond), which could influence binding, resulting in tighter binding to the CAR receptor. Asparagine 165 and Valine 199 are the protein residues to which β-Sitosterol and Ursodeoxycholic acid bind, respectively. The metabolites extracted from *B. carteri* were docked to the PXR receptor, using Rifampicin as a control for bonding. Hydrogen bonding was demonstrated by Trans-4',5-dihydroxy-3-methoxystilbene-5-O-[α-l-rhamnopyranosyl-(1→6)]-β-d-glucopyranoside with Serine 247, Lysine 210, and Glycine 285; and Boswellic acid with Glycine 285. Based on the earlier information, it showed that Boswellic acid has only one hydrogen bond, even though it has the lowest docking score, showing a higher affinity

toward PXR compared to Trans-4',5-dihydroxy-3-methoxystilbene-5-O-[α-l-rhamnopyranosyl-(1→6)]-β-d-glucopyranoside and Rifampicin. Trans-4',5-dihydroxy-3-methoxystilbene-5-O-[α-l-rhamnopyranosyl-(1→6)]-β-d-glucopyranoside has three hydrogen bonds, and the docking score was modest between Rifampicin, which has the highest docking score, and Boswellic acid that has the lowest docking score. Finally, both CAR and PXR receptors displayed binding to two metabolites, showing a potential effect on the receptors present in the CYP-450 isoenzyme subtypes 1A2, 2B6,3A4.

PXR and CAR Binding by B. carteri Metabolites

To complement the in silico docking results, we measured the binding interactions of *B. carteri* aqueous extract metabolites with two nuclear receptors, PXR and CAR. Rifampicin competitively binds to human PXR, and Rifampicin is reported to be a strong agonist ligand for human PXR.[57,58] Although Trans-4',5-dihydroxy-3-methoxystilbene-5-O-[α-l-rhamnopyranosyl-(1→6)]-β-d-glucopyranoside and Boswellic acid showed an acceptable binding affinity to the PXR receptor in docking studies, the experimental results did not reflect significant binding activity. This discrepancy may be attributed to varying concentrations of these molecules in the aqueous extracts of *Boswellia carteri* resin, which could have ultimately influenced the experimental outcomes. CITCO was used as an agonist control for the CAR binding assay with an agonist-mode curve. Both *B. carteri* resin aqueous extracts contained agonist(s) for CAR, which may explain the increase in CYP 2B6 and 3A4 enzyme gene expression. CAR activation induces both human CYP 2B6 and 3A4 enzyme gene expression.[59,60] This agrees with the study results that both β-sitosterol and ursodeoxycholic acid show high docking scores with the human CAR crystal structure. Although the observed increase in CYP 1A2 enzyme gene expression could be attributed to the binding of *B. carteri* resin metabolites to the AhR receptor, there is evidence that CYP 1A2 can be induced by the activation of CAR receptor.[61,62] Further studies are needed to determine whether the induction of CYP1A2 gene expression is due to AhR activation.

It should be noted that this study has limitations to represent the actual clinical situation. This includes the assumption that all bioactive present in the *B. carteri* resin extract mixture is absorbed into the body system and reach the biological target(s). Another limitation worth mentioning is that the presence and amount of bioactive(s) do differ from one plant to another, and thus difference in CYP modulation might be observed from one harvest lot to another of *B. carteri* resins. Thus, the modulation effect might be stronger from the lot used in this study. Furthermore, in vivo chemical mixture interaction between *B. carteri* constituent(s) might result in different modulation effects in comparison to in vitro results. All together, caution should be exercised when extrapolating this study's results to represent the actual clinical herb–drug interaction situation. Nevertheless, this study warns patients and consumers about the repeated concomitant consumption of *B. carteri* resins and pharmaceutical drugs.

Conclusions

B. carteri resin extraction showed its utility for inducing specific CYP enzyme subtypes, which are 1A2, 2B6, and 3A4. In vitro *studies* have shown that *B. carteri* resin extracts can induce the gene expression of CYP enzymes, particularly through CAR nuclear receptors. Moreover, the PXR receptor is a potential target for modulating CYP enzyme induction. In silico studies have also illustrated that *B. carteri* extracted metabolites bind to CAR and PXR receptors, which modulate the gene expression of CYP enzyme subtypes and thereby induce CYP enzyme expression. Our study emphasizes that CYP enzyme induction mediated by *B. carteri* plant extracts could potentially increase the likelihood of drug-herbal interactions.

Abbreviations

ADME, Absorption, Distribution, Metabolism, and Excretion; AhR, Aryl Hydrocarbon Receptor; *B. carteri, Boswellia carteri* Resin; CAR, Constitutive Androstane Receptor; cDNA, Complementary DNA; CO_2, Carbon Dioxide; CYP, Cytochrome P-450; DMEM, Dulbecco's Modified Eagle Medium; DMSO, Dimethyl Sulfoxide; DNA, Deoxyribonucleic Acid; EC_{50}, Effective Concentration; EU, Endotoxin Unit; Hep G2, Human Hepatocellular Carcinoma Cell Line; FBS, Fetal Bovine Serum; GAPDH, Glyceraldehyde-3-phosphate Dehydrogenase; LC/MS, Liquid Chromatography and Mass Spectrometry; $LD_{50,}$ Lethal Dose; MFE, Molecular Features Extraction; MTT, 3-[4,5-Dimethylthiazol-2-yl]-2,5-diphenyltetrazolium bromide; PASS, Prediction of Activity Spectra for Substances; PBS, Phosphate-Buffered Saline; PXR,

Pregnane X Receptor; QTOF, Time-Of-Flight; RNA, Ribonucleic Acid; RT-qPCR, Reverse Transcription-Quantitative Polymerase Chain Reaction; US FDA, United States Food and Drug Administration.

Data Sharing Statement

The data presented in this study are available on request from the corresponding author.

Acknowledgments

The authors express their sincere gratitude to the College of Pharmacy (COP) at King Saud bin Abdulaziz University for Health Sciences (KSAU-HS) for their continued support. We would also like to thank Dr. Feras Almourfi for helping us with the LCMS experiment.

Author Contributions

All authors made a significant contribution to the work reported, whether that is in the conception, study design, execution, acquisition of data, analysis and interpretation, or in all these areas; took part in drafting, revising, or critically reviewing the article; gave final approval of the version to be published; have agreed on the journal to which the article has been submitted; and agree to be accountable for all aspects of the work.

Funding

This research was funded by the King Abdullah International Medical Research Center (KAIMRC), Ministry of National Guard Health Affairs, Riyadh, and the Kingdom of Saudi Arabia (SP22R-054-04).

Disclosure

The authors declare that this research was conducted in the absence of any commercial or financial relationships that could be construed as potential conflicts of interest.

References

1. DeCarlo A, Johnson S, Poudel A, Satyal P, Bangerter L, Setzer WN. Chemical variation in essential oils from the oleo-gum resin of boswellia carteri: a preliminary investigation. *Chem Biodivers*. 2018;15(6):e1800047. doi:10.1002/cbdv.201800047
2. Khalifa SAM, Kotb SM, El-Seedi SH, et al. Frankincense of *Boswellia sacra*: traditional and modern applied uses, pharmacological activities, and clinical trials. *Ind Crops Prod*. 2023;203:117106. doi:10.1016/j.indcrop.2023.117106
3. Moussaieff A, Mechoulam R. Boswellia resin: from religious ceremonies to medical uses; a review of in-vitro, in-vivo and clinical trials. *J Pharm Pharmacol*. 2009;61(10):1281–1293. doi:10.1211/jpp.61.10.0003
4. Yoon JH, Kim JH, Ham SS, et al. Optimal processing conditions of Boswellia carteri Birdw. using response surface methodology. *Pharmacogn Mag*. 2018;14(54):235. doi:10.4103/pm.pm_140_17
5. Badria FA, Mikhaeil BR, Maatooq GT, Amer MMA. Immunomodulatory triterpenoids from the oleogum resin of Boswellia carterii Birdwood. *Z Naturforschung C J Biosci*. 2003;58(7–8):505–516. doi:10.1515/znc-2003-7-811
6. Antioxidant, antimicrobial, and anti-insect properties of boswellia carterii essential oil for food preservation improvement. Available from: https://www.mdpi.com/2311-7524/9/3/333. Accessed December 22, 2024.
7. Hasson SO, Jasim AM, Salman SAK, Akrami S, Saki M, Hassan MA. Evaluation of antibacterial and wound-healing activities of alcoholic extract of Boswellia carterii, in vitro and in vivo study. *J Cosmet Dermatol*. 2022;21(11):6199–6208. doi:10.1111/jocd.15206
8. Koshak AE. Prevalence of herbal medicines in patients with chronic allergic disorders in Western Saudi Arabia. *Saudi Med J*. 2019;40(4):391–396. doi:10.15537/smj.2019.4.24006
9. Alamoudi A, Alrefaey Y, Asiri Y, et al. Pattern and factors associated with the utilization of herbs as medications among patients in a tertiary care hospital in Western Saudi Arabia. *Cureus*. 2021;13(11). doi:10.7759/cureus.19502
10. Rombolà L, Scuteri D, Marilisa S, et al. Pharmacokinetic interactions between herbal medicines and drugs: their mechanisms and clinical relevance. *Life*. 2020;10(7):106. doi:10.3390/life10070106
11. Esteves F, Rueff J, Kranendonk M. The central role of cytochrome P450 in xenobiotic metabolism-A brief review on a fascinating enzyme family. *J Xenobiotics*. 2021;11(3):94–114. doi:10.3390/jox11030007
12. Fuhr U. Induction of drug metabolising enzymes: pharmacokinetic and toxicological consequences in humans. *Clin Pharmacokinet*. 2000;38(6):493–504. doi:10.2165/00003088-200038060-00003
13. Rakateli L, Huchzermeier R, van der Vorst EPCA. PXR and CAR: from xenobiotic receptors to metabolic sensors. *Cells*. 2023;12(23):2752. doi:10.3390/cells12232752
14. Xu C, Li CYT, Kong ANT. Induction of Phase I, II and III drug metabolism/transport by xenobiotics. *Arch Pharm Res*. 2005;28(3):249–268. doi:10.1007/BF02977789

15. Gendy M, El-Kadi A, Peganum Harmala L. Differentially modulates cytochrome P450 gene expression in human hepatoma HepG2 cells. *Drug Metab Lett*. 2009;3:212–216. doi:10.2174/187231209790218163
16. Alehaideb Z, Alatar G, Nehdi A, et al. Commiphora myrrha (Nees) Engl. resin extracts induce phase-I cytochrome P450 2C8, 2C9, 2C19, and 3A4 isoenzyme expressions in human hepatocellular carcinoma (HepG2) cells. *Saudi Pharm J SPJ off Publ Saudi Pharm Soc*. 2021;29(5):361–368. doi:10.1016/j.jsps.2021.03.002
17. Filimonov DA, Lagunin AA, Gloriozova TA, et al. Prediction of the biological activity spectra of organic compounds using the pass online web resource. *Chem Heterocycl Compd*. 2014;50(3):444–457. doi:10.1007/s10593-014-1496-1
18. Nickel J, Gohlke BO, Erehman J, et al. SuperPred: update on drug classification and target prediction. *Nucleic Acids Res*. 2014;42(W1):W26–W31. doi:10.1093/nar/gku477
19. Gfeller D, Grosdidier A, Wirth M, Daina A, Michielin O, Zoete V. SwissTargetPrediction: a web server for target prediction of bioactive small molecules. *Nucleic Acids Res*. 2014;42(W1):W32–W38. doi:10.1093/nar/gku293
20. Daina A, Michielin O, Zoete V. SwissADME: a free web tool to evaluate pharmacokinetics, drug-likeness and medicinal chemistry friendliness of small molecules. *Sci Rep*. 2017;7(1):42717. doi:10.1038/srep42717
21. B-Rao C, Kulkarni-Almeida A, Katkar KV, et al. Identification of novel isocytosine derivatives as xanthine oxidase inhibitors from a set of virtual screening hits. *Bioorg Med Chem*. 2012;20(9):2930–2939. doi:10.1016/j.bmc.2012.03.019
22. Banerjee P, Eckert AO, Schrey AK, Preissner R. ProTox-II: a webserver for the prediction of toxicity of chemicals. *Nucleic Acids Res*. 2018;46 (Web Server issue):. doi:10.1093/nar/gky318
23. Iftkhar S, de Sá AGC, Velloso JPL, Aljarf R, Pires DEV, Ascher DB. cardioToxCSM: a web server for predicting cardiotoxicity of small molecules. *J Chem Inf Model*. 2022;62(20):4827–4836. doi:10.1021/acs.jcim.2c00822
24. RCSB PDB: homepage. Available from: https://www.rcsb.org/#Category-deposit. Accessed December 24, 2024.
25. Wang F, Li ZL, Cui HH, Hua HM, Jing YK, Liang SW. Two new triterpenoids from the resin of Boswellia carterii. *J Asian Nat Prod Res*. 2011;13 (3):193–197. doi:10.1080/10286020.2010.548808
26. Ammon HPT. Modulation of the immune system by Boswellia serrata extracts and boswellic acids. *Phytomedicine Int J Phytother Phytopharm*. 2010;17(11):862–867. doi:10.1016/j.phymed.2010.03.003
27. Yang X, Wu X. Revaluation of Xihuang Pill on tumor treatment: from ancient literatures to modern studies. *Tradit Med Res*. 2016;1(2):60–74. doi:10.53388/TMR201602009
28. Atta-ur-Rahman, Naz H, Fadimatou, et al. Bioactive constituents from Boswellia papyrifera. *J Nat Prod*. 2005;68(2):189–193. doi:10.1021/np040142x
29. Mannino G, Occhipinti A, Maffei ME. Quantitative determination of 3-O-Acetyl-11-Keto-βBoswellic acid (AKBA) and other boswellic acids in Boswellia sacra Flueck (syn. B. carteri Birdw) and Boswellia serrata Roxb. *Mol*. 2016;21(10):1329. doi:10.3390/molecules21101329
30. Goel RK, Singh D, Lagunin A, Poroikov V. PASS-assisted exploration of new therapeutic potential of natural products. *Med Chem Res*. 2011;20 (9):1509–1514. doi:10.1007/s00044-010-9398-y
31. Kumar S. Computational identification and binding analysis of orphan human cytochrome P450 4X1 enzyme with substrates. *BMC Res Notes*. 2015;8(1):9. doi:10.1186/s13104-015-0976-4
32. Hemaiswarya S, Prabhakar PK, Doble M. Synergistic Herb Interactions with Anticancer Drugs. In: Hemaiswarya S, Prabhakar PK, Doble M editors. *Herb-Drug Combinations: A New Complementary Therapeutic Strategy*. Springer Nature; 2022:145–173. doi:10.1007/978-981-19-5125-1_10.
33. Drwal MN, Banerjee P, Dunkel M, Wettig MR, Preissner R. ProTox: a web server for the in silico prediction of rodent oral toxicity. *Nucleic Acids Res*. 2014. 42. doi:10.1093/nar/gku401
34. Ekor M. The growing use of herbal medicines: issues relating to adverse reactions and challenges in monitoring safety. *Front Pharmacol*. 2014;4:177. doi:10.3389/fphar.2013.00177
35. Tulunay M, Aypak C, Yikilkan H, Gorpelioglu S. Herbal medicine use among patients with chronic diseases. *J Intercult Ethnopharmacol*. 2015;4 (3):217–220. doi:10.5455/jice.20150623090040
36. Damery S, Gratus C, Grieve R, et al. The use of herbal medicines by people with cancer: a cross-sectional survey. *Br J Cancer*. 2011;104 (6):927–933. doi:10.1038/bjc.2011.47
37. Kajiyama S, Shoji T, Okuda S, Izumi Y, Ichiro FE, Kobayashi A. A novel microsurgery method for intact plant tissue at the single cell level using ArF excimer laser microprojection. *Biotechnol Bioeng*. 2006;93(2):325–331. doi:10.1002/bit.20709
38. Liu TG, Xiong SQ, Yan Y, Zhu H, Yi C. Use of Chinese herb medicine in cancer patients: a survey in Southwestern China. *Evid Based Complement Alternat Med*. 2012;2012(1):769042. doi:10.1155/2012/769042
39. Alghadir AH, Iqbal A, Iqbal ZA. Attitude, beliefs, and use of herbal remedies by patients in the Riyadh Region of Saudi Arabia. *Healthcare*. 2022;10(5):907. doi:10.3390/healthcare10050907
40. Alghamdi M, Mohammed A, Alfahaid F, Albshabshe A. Herbal medicine use by Saudi patients with chronic diseases: a cross-sectional study (experience from Southern Region of Saudi Arabia). *J Health Spec*. 2018;6:77. doi:10.4103/jhs.JHS_157_17
41. Dayyih WA, Al-Ani I, Hailat M, et al. Review of grapefruit juice-drugs interactions mediated by intestinal CYP3A4 inhibition. *J Appl Pharm Sci*. 2024;14(5):059–068. doi:10.7324/JAPS.2024.160197
42. Hohmann N, Friedrichs AS, Burhenne J, Blank A, Mikus G, Haefeli WE. Dose-dependent induction of CYP3A activity by St. John's wort alone and in combination with rifampin. *Clin Transl Sci*. 2024;17(8):e70007. doi:10.1111/cts.70007
43. Butash KA, Natarajan P, Young A, Fox DK. Reexamination of the effect of endotoxin on cell proliferation and transfection efficiency. *BioTechniques*. 2000;29(3):610–614,616,618–619. doi:10.2144/00293rr04
44. Shedlofsky SI, Israel BC, McClain CJ, Hill DB, Blouin RA. Endotoxin administration to humans inhibits hepatic cytochrome P450-mediated drug metabolism. *J Clin Invest*. 1994;94(6):2209–2214.
45. Westerink WMA, Schoonen WGEJ. Cytochrome P450 enzyme levels in HepG2 cells and cryopreserved primary human hepatocytes and their induction in HepG2 cells. *Toxicol Vitro Int J Publ Assoc BIBRA*. 2007;21(8):1581–1591. doi:10.1016/j.tiv.2007.05.014
46. HepG2 cells as an in vitro model for evaluation of cytochrome P450 induction by xenobiotics - PubMed. Available from: https://pubmed.ncbi.nlm.nih.gov/25336106/. Accessed December 22, 2024.

47. Sinz M, Wallace G, Sahi J. Current industrial practices in assessing CYP450 Enzyme induction: preclinical and clinical. *AAPS J*. 2008;10(2):391–400. doi:10.1208/s12248-008-9037-4
48. US FDA. 2020. Available from: https://www.fda.gov/media/134582/download. Accessed August 14, 2024.
49. Faucette SR, Wang H, Hamilton GA, et al. Regulation of Cyp2b6 in primary human hepatocytes by prototypical inducers. *Drug Metab Dispos*. 2004;32(3):348–358. doi:10.1124/dmd.32.3.348
50. Rekić D, Röshammar D, Mukonzo J, Ashton M. In silico prediction of efavirenz and rifampicin drug–drug interaction considering weight and CYP2B6 phenotype. *Br J Clin Pharmacol*. 2011;71(4):536–543. doi:10.1111/j.1365-2125.2010.03883.x
51. Backman JT, Granfors MT, Neuvonen PJ. Rifampicin is only a weak inducer of CYP1A2-mediated presystemic and systemic metabolism: studies with tizanidine and caffeine. *Eur J Clin Pharmacol*. 2006;62(6):451–461. doi:10.1007/s00228-006-0127-x
52. Kanebratt KP, Andersson TB. Evaluation of HepaRG cells as an in vitro model for human drug metabolism studies. *Drug Metab Dispos Biol Fate Chem*. 2008;36(7):1444–1452. doi:10.1124/dmd.107.020016
53. Hempfling W, Dilger K, Beuers U. Ursodeoxycholic acid — adverse effects and drug interactions. *Aliment Pharmacol Ther*. 2003;18(10):963–972. doi:10.1046/j.1365-2036.2003.01792.x
54. Yu J, Wang L, Ding J, Wu L. Extraction of oleic acid from animals oil and its anti-inflammatory effect on network pharmacology. *Iran J Sci Technol Trans Sci*. 2021;45(6):1905–1913. doi:10.1007/s40995-021-01168-3
55. Jairaman C, Alehaideb ZI, Yacoob SAM, et al. Rhizophora mucronata Lam. (Mangrove) Bark extract reduces ethanol-induced liver cell death and oxidative stress in Swiss albino mice: in vivo and in silico studies. *Metabolites*. 2022;12(11):1021. doi:10.3390/metabo12111021
56. Huang K, Chen Y, Liang K, et al. Review of the chemical composition, pharmacological effects, pharmacokinetics, and quality control of Boswellia carterii. *Evid-Based Compl Altern Med ECAM*. 2022;2022:6627104. doi:10.1155/2022/6627104
57. Li T, Chiang JYL. Rifampicin induction of CYP3A4 requires pregnane x receptor cross talk with hepatocyte nuclear factor 4α and coactivators, and suppression of small heterodimer partner gene expression. *Drug Metab Dispos*. 2006;34(5):756–764. doi:10.1124/dmd.105.007575
58. Yamasaki Y, Kobayashi K, Inaba A, et al. Indirect activation of pregnane X receptor in the induction of hepatic CYP3A11 by high-dose rifampicin in mice. *Xenobiotica*. 2018;48(11):1098–1105. doi:10.1080/00498254.2017.1400128
59. Goodwin B, Redinbo MR, Kliewer SA. Regulation of cyp3a gene transcription by the pregnane x receptor. *Annu Rev Pharmacol Toxicol*. 2002;42:1–23. doi:10.1146/annurev.pharmtox.42.111901.111051
60. Kliewer SA, Goodwin B, Willson TM. The nuclear pregnane X receptor: a key regulator of xenobiotic metabolism. *Endocr Rev*. 2002;23(5):687–702. doi:10.1210/er.2001-0038
61. Tojima H, Kakizaki S, Yamazaki Y, et al. Ligand dependent hepatic gene expression profiles of nuclear receptors CAR and PXR. *Toxicol Lett*. 2012;212(3):288–297. doi:10.1016/j.toxlet.2012.06.001
62. Tolson AH, Wang H. Regulation of drug-metabolizing enzymes by xenobiotic receptors: PXR and CAR. *Adv Drug Deliv Rev*. 2010;62(13):1238–1249. doi:10.1016/j.addr.2010.08.006

Biologics: Targets and Therapy

Dovepress
Taylor & Francis Group

Publish your work in this journal

Biologics: Targets and Therapy is an international, peer-reviewed journal focusing on the patho-physiological rationale for and clinical application of Biologic agents in the management of autoimmune diseases, cancers or other pathologies where a molecular target can be identified. This journal is indexed on PubMed Central, CAS, EMBase, Scopus and the Elsevier Bibliographic databases. The manuscript management system is completely online and includes a very quick and fair peer-review system, which is all easy to use. Visit http://www.dovepress.com/testimonials.php to read real quotes from published authors.

Submit your manuscript here: https://www.dovepress.com/biologics-targets-and-therapy-journal